livers

MDPI

Review

Human-Mouse Convergence in Metabolic Dysfunction-Associated Steatotic Liver Disease: Mouse Model Selection and Non-Invasive Diagnostic Strategies

Denise Bonente [1,2,†], Sara Gargiulo [3,†], Ludovica Livi [4], Matteo Gramanzini [5], Tiziana Tamborrino [1,2], Lisa Gherardini [3], Giovanni Inzalaco [6], Lorenzo Franci [7], Mario Chiariello [3,8] and Virginia Barone [1,*]

1 Department of Molecular and Developmental Medicine, University of Siena, 53100 Siena, Italy; denise.bonente2@unisi.it (D.B.); tiziana.tamborrino@student.unisi.it (T.T.)
2 Department of Life Sciences, University of Siena, 53100 Siena, Italy
3 Institute of Clinical Physiology, National Research Council, Via Fiorentina 1, 53100 Siena, Italy; sara.gargiulo@cnr.it (S.G.); lisa.gherardini@cnr.it (L.G.); mario.chiariello@cnr.it (M.C.)
4 Department of Medical, Surgical and Neurological Science, University of Siena, 53100 Siena, Italy; ludovicalivi@gmail.com
5 Institute of Crystallography, National Research Council, Strada Provinciale 35d, n. 9-00010, Montelibretti, 00010 Rome, Italy; matteo.gramanzini@cnr.it
6 Institute of Endotypes in Oncology, Metabolism and Immunology "Gaetano Salvatore", National Research Council, Via Pansini 5, 80131 Napoli, Italy; giovanniinzalaco@cnr.it
7 Department of Industrial Chemistry "Toso Montanari", University of Bologna, 40136 Bologna, Italy; lorenzo.franci3@unibo.it
8 Core Research Laboratory, Istituto per lo Studio, la Prevenzione e la Rete Oncologica, 53100 Siena, Italy
* Correspondence: virginia.barone@unisi.it; Tel.: +39-0577-232053
† These authors contributed equally to this work.

Abstract

Background: Metabolic Dysfunction-Associated Steatotic Liver Disease (MASLD) is a global health priority affecting approximately 30% of the population. It represents the hepatic manifestation of metabolic syndrome, potentially progressing from simple steatosis to Metabolic Dysfunction-Associated Steatohepatitis (MASH), cirrhosis, and hepatocellular carcinoma. This review aims to compare current knowledge of MASLD in mouse models and humans, focusing on pathophysiology, histological phenotypes, and the role of preclinical imaging as a non-invasive translational screening tool. **Methods:** A literature search was conducted in PubMed and Web of Science to identify English-language publications from January 2020 to March 2026 on murine models and imaging techniques for MASLD, using pertinent keywords. Attention was given to highlighting similarities and differences between human and murine approaches. **Results:** MASLD arises from complex interactions between genetics, sedentary lifestyles, and imbalanced diets. While mouse models have been refined to capture the multifactorial interplay driving disease progression and are still essential for drug development, no single model fully mirrors the human condition. Histological assessment remains an essential tool for MASLD staging, in both humans and mouse models. However, imaging is increasingly emerging as an important complementary technique to non-invasively investigate MASLD. **Conclusions:** Mouse models are essential to address specific mechanistic and therapeutic questions, but understanding of their limitations and strengths is crucial for translational research. Integrating phenotype-driven approaches in both humans and mice, combining traditional histology, quantitative imaging, and metabolic profiling, as well as longitudinal, combined, and humanized preclinical models, will enhance translational alignment and accelerate the development of therapies for MASLD.

Check for updates

Received: 11 February 2026
Revised: 22 April 2026
Accepted: 22 May 2026
Published: 1 June 2026

Copyright: © 2026 by the authors. Licensee MDPI, Basel, Switzerland. This article is an open access article distributed under the terms and conditions of the Creative Commons Attribution (CC BY) license.

Keywords: Metabolic Dysfunction-Associated Steatotic Liver Disease; Non-Alcoholic Fatty Liver Disease; MASLD; hepatic steatosis; mouse models; non-invasive imaging

1. Hepatic Steatosis and Metabolic Dysfunction-Associated Steatotic Liver Disease (MASLD): Overview

1.1. MASLD Landscape: Pathogenesis and Diagnosis

Hepatic steatosis is defined as the presence of intrahepatic fat, accounting for at least 5% of total liver weight [1]. It can be caused by excessive alcohol consumption, where it represents one of the main features observed in alcoholic liver diseases (ALDs), or by metabolic factors like obesity, insulin resistance (IR), and dyslipidemia. This second condition, named Metabolic Dysfunction-Associated Steatotic Liver Disease (MASLD, previously known as Non-Alcoholic Fatty Liver Disease—NAFLD), has gained much attention in recent years due to its potential to progress to more severe forms [2]. MASLD is considered the hepatic manifestation of metabolic syndrome, encompassing a spectrum of conditions that range from a simple and relatively benign form of hepatic fat accumulation to a more severe form of Metabolic Dysfunction–Associated SteatoHepatitis (MASH), characterized by inflammation, iron deposition, hepatocellular damage, and fibrosis, which may ultimately progress to cirrhosis and hepatocellular carcinoma (HCC) [3,4].

Its global prevalence is very high, affecting approximately 30% of the population, and its incidence has increased by 50.4% from 1990 to the present [5]. In MASLD, hepatic steatosis is associated with at least one cardiometabolic risk factor, including hyperlipidemia, hyperglycemia, IR, and overweight [2]. MASLD has been frequently considered a condition closely linked to obesity, but it is now increasingly appreciated in individuals with a normal body mass index (BMI), a condition known as "lean MASLD" [6]. Indeed, MASLD is a multifactorial disease whose pathophysiology is not yet fully understood, arising from a combination of genetic predisposition, dietary factors, sedentary lifestyle, and gut dysbiosis [7].

Genetic factors play a significant role in MASLD, with variants identified in genes that regulate glucose and fat regulatory pathways. For example, the rs738409 (c.444C>G) polymorphism in the patatin-like phospholipase domain-containing 3 (*PNPLA3*) gene is present in 30–50% of individuals with MASLD. This variant leads to an isoleucine-to-methionine substitution at position 148 (p.I148M), resulting in increased hepatic lipid retention during feeding and excessive lipid oxidation during fasting. These alterations overwhelm hepatocytes' metabolic capacity and ultimately promote cellular toxicity, leading to hepatic damage [8]. Another well-known polymorphism is the *HSD17B13* variant of 17β-hydroxysteroid dehydrogenase-13, which is a hepatocyte-specific, lipid droplet-associated protein. *HSD17B13* gene expression and protein levels are upregulated in MASLD-affected patients, and overexpression of *Hsd17b13* in mice promotes rapid lipid accumulation in the liver [9]. Also, the missense variant rs1260326 (p.P446L) and the intronic variant rs780094 of the glucokinase regulatory protein gene (*GCRK*) are associated with increased de novo lipogenesis and higher plasma triglyceride levels [10]. Single-nucleotide polymorphisms in membrane-bound O-acyltransferase domain–containing 7 (*MBOAT7*) are associated with increased risk of initiation and progression of MASLD and fibrosis; indeed, multiple in vitro and in vivo studies showed how *MBOAT7* deficiency in mice and humans alters the hepatic phospholipid composition and promotes hyperinsulinemia and hepatic IR [11]. Lastly, the rs58542926 variant in the *TM6SF2* gene (p.E167K), by inhibiting the secretion of very low-density lipoproteins from hepatocytes, promotes triglyceride accumulation within the liver parenchyma [12].

An imbalanced diet is another risk factor for MASLD. This involves alterations in both macro- and micronutrient intake, characterized not only by increased consumption of calories, i.e., simple carbohydrates, cholesterol, and total saturated fatty acids, but also by excessive selenium and reduced vitamins K and E intakes. Such dietary patterns promote IR and hepatic lipid accumulation, and a positive correlation has been observed between circulating selenium levels and liver fibrosis. Conversely, deficiencies in vitamins E and K contribute to increased oxidative stress and impaired glycemic control [13].

In particular, a diet rich in simple sugars but low in fiber has been implicated in the development of MASLD through several mechanisms, including alterations in the composition and function of the gut microbiota [14,15]. Patients with MASLD frequently exhibit an imbalanced gut microbiota, characterized by an overrepresentation of Proteobacteria and Fusobacteria phyla that include many opportunistic pathogens, and a concomitant reduction in protective genera such as *Prevotella* and *Faecalibacterium*. This could compromise gut barrier integrity and the production of short-chain fatty acids, leading to gut leakiness and chronic inflammation [16].

Along with unbalanced dietary habits, individuals with MASLD tend to be more sedentary, while regular physical activity has been shown to be effective in preventing the onset of MASLD [13]. Indeed, emerging evidence supports the existence of a muscle–liver crosstalk, whereby myokines released by muscles during physical activity, such as decorin and IL-6, promote mitochondrial fatty acid β-oxidation, mitigating diet-induced hepatic steatosis and attenuating hepatic inflammation [17,18].

Given its multifactorial etiology, MASLD remains a therapeutic challenge. Current management strategies primarily focus on dietary modifications, increased physical activity, and pharmacological interventions with drugs such as Pioglitazone, Vitamin E, and antagonists of the glucagon-like peptide-receptor 1 (GLP-1R) and peroxisome proliferator–activated receptor (PPAR) [19]. In this context, experimental mouse models of MASLD play a fundamental role, as they enable detailed investigation of the disease's pathophysiology and may help uncover new pathways that could serve as therapeutic targets. Moreover, mouse strains have diverse genetic backgrounds and are susceptible to genetic manipulation, which helps to identify the genetic factors underlying MASLD. Compared to animal models with more developed brain functions, mice can model varying degrees of MASLD based on environmental, genetic, and epigenetic factors or their combination, with ease of management, shorter investigation times, lower costs, and fewer ethical concerns.

In both humans and mice, MASLD is currently confirmed and staged by using histology as the reference method; however, non-invasive diagnostic and imaging approaches are increasingly recommended. In the clinical setting, recent advances in imaging enable safer image-guided liver biopsies and support integrated MASLD screening strategies for early diagnosis in high-risk patients or when biopsy is contraindicated due to underlying health conditions [20,21]. In the preclinical setting, histological assessment of MASLD requires animal sacrifice, thereby precluding longitudinal evaluation of disease progression or therapeutic response within the same subject and increasing the number of animals used at multiple experimental time points [22]. Therefore, the implementation of preclinical imaging approaches is highly relevant and translationally valuable for MASLD research, as it complements invasive methods while addressing both scientific and ethical concerns.

Considering these aspects, the purpose of this narrative review is to provide a contemporary overview of the refinements of genetic and/or dietary MASLD mouse models in the last five-year publications, highlighting the varied and controversial efforts to reproduce the full spectrum of MASLD outcomes, including metabolic alterations, hepatic inflammation, and fibrosis. We reviewed their comparability to humans and translational relevance, focusing on current histopathological evidence for MASLD/MASH in murine

models and advances in preclinical imaging, highlighting key cutting-edge factors that need to be considered when choosing a specific mouse model.

1.2. Data Sources and Searches

We conducted an extensive literature search of eligible English-language publications from PubMed and Web of Science to gather the most recent and relevant preclinical studies, clinical guidelines, and expert recommendations.

The search strategy was adapted for narrative synthesis with coverage from January 2020 up to March 2026, using the following keywords combined by Boolean operators (e.g., AND, OR): non-alcoholic fatty liver disease, NAFLD, metabolic-associated steatotic liver disease, MASLD, non-alcoholic steatohepatitis, metabolic-associated steatohepatitis, MASH, hepatic steatosis, mouse model, diet induced, genetically modified mice, preclinical imaging, liver imaging, liver ultrasound, liver MRI, comparative histology.

Bibliographies of relevant articles were also examined to identify additional sources. Original research articles and narrative or systematic reviews were included, while other types of publications, whether in different languages or concerning ALD, were excluded.

2. Mouse Models of MASLD: Strengths and Pitfalls in Comparative Pathology

2.1. Current Evidence from Diet-Induced Mouse Models of MASLD

Given the complexity of MASLD pathophysiology and interspecies differences in liver biology, neither cellular systems nor animal models can completely reproduce the human disease. Despite advances, both simpler 2D cell cultures, such as HepG2 and Huh7, and 3D organoids derived from human cells are still unable to fully replicate the metabolism of hepatocytes in living organisms [23–26]. Laboratory mice are the most widely used animal models for studying MASLD. Although mice exhibit liver anatomy similar to humans, they also show pathophysiological differences in their transcriptome, enzymatic activities, and lipoprotein profile and transport [27,28].

Over the past decades, several mouse models have been developed to study the pathogenesis and treatment of MASLD. Extensive reviews have described the most well-established models induced by diet, genetic modifications, and chemicals. High fat diet (HFD), methionine and/or choline deficient diet (MCD/CD), cafeteria diet (CAFD) and western diet (WD), or chemicals such as carbon tetrachloride, streptozocin or exposure to cigarette smoke, have been used in different settings on mouse strains susceptible to metabolic syndrome (C57BL/6, FVB/N, DBA/2J, 129S1/SvlmJ) or genetically engineered mouse models (GEMs) (ob/ob, db/db, *LDLR*−/−, *ApoE*−/−) or knock-out (KO) mice for the targeted genes of interest [29–33]. However, further refinements are underway to improve the understanding of the complex interplay between genetic, metabolic, and environmental factors that drive disease development and progression. Mouse models representing the early stages of MASLD help study the etiopathogenesis of simple steatosis. They are valuable for testing preventive strategies in a still reversible, but often underdiagnosed, pathological state, as recently highlighted by the LITMUS consortium. Conversely, late-stage mouse models are essential for studying the transition to more advanced disease stages, such as inflammation, fibrosis, and cancer [34,35].

Selecting the most suitable MASLD model requires a balance between a model's ability to address a particular experimental question and its limitations in representing the full spectrum of human MASLD. Several factors must be considered, including diet selection, mouse strains, the use of GEMs, and housing conditions (Figure 1).

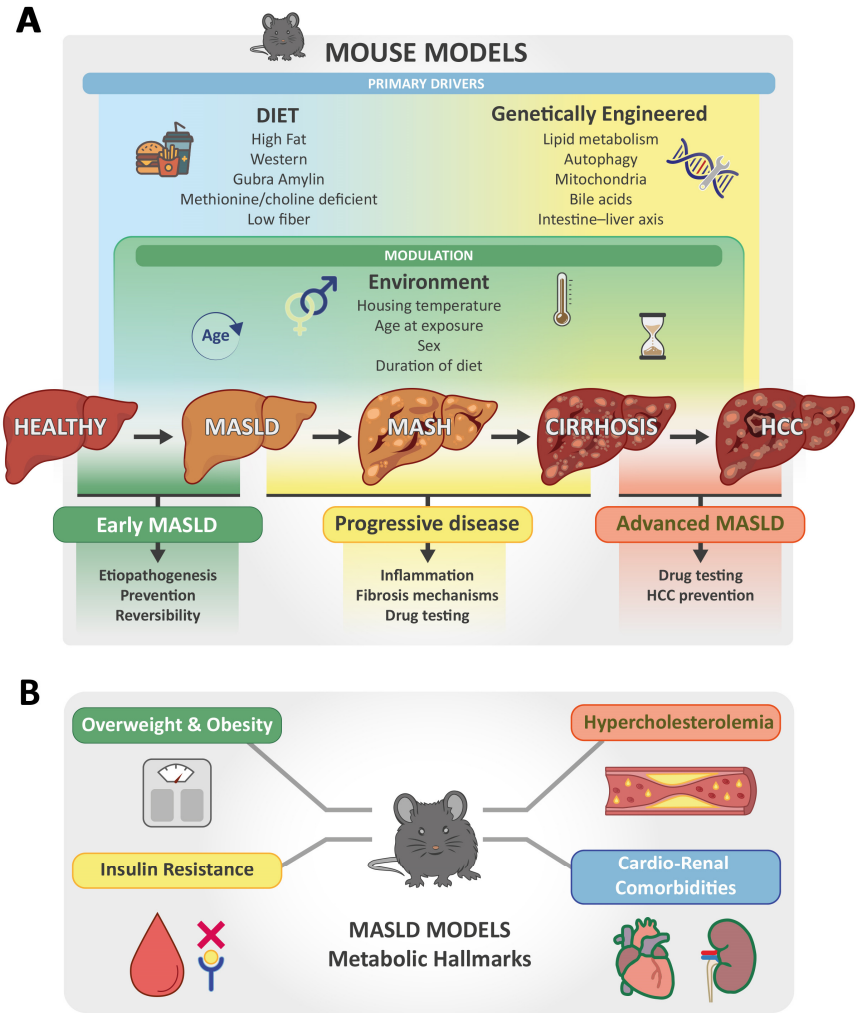

Figure 1. Mouse models: modeling of disease stages and translational relevance. (**A**) The figure provides a visual framework for understanding how mouse models can reproduce different outcomes of the MASLD spectrum. The central axis represents disease progression from reversible hepatic steatosis to more severe conditions of MASH, fibrosis, and HCC. Above the axis, the main experimental drivers are depicted: type of diet and its duration primarily determine disease progression, while genetic background and engineered models modulate key pathways such as lipid metabolism, autophagy, mitochondrial function, bile acid regulation, and gut–liver interactions. Age, sex, and housing temperature further influence disease severity. Below the spectrum, the figure links disease stages to their typical experimental applications, from studies on etiopathogenesis and prevention in early MASLD to investigations of inflammation, fibrosis, and therapeutic testing in advanced stages. (**B**) Schematic representation of the key metabolic phenotypes and health risk factors observed in mouse models of MASLD, including obesity, insulin resistance, hypercholesterolemia, and cardio-renal complications.

Variations in diet composition and duration can strongly influence metabolic phenotypes and pathological outcomes in mouse models. Still, diets that differ significantly from human eating patterns often lead to poor transferability of results [36]. Conversely, mouse models subjected to WDs that develop features of metabolic syndrome, including severe obesity, hypercholesterolemia, hyperinsulinemia, IR, and cardiorenal comorbidities, are valuable for improving translational research [36].

Current medical research strongly supports the link between MASLD and dietary patterns based on processed foods widely consumed in Western countries, which are high in saturated fat, cholesterol, and simple sugars (particularly fructose and sucrose), but low in fiber and high-quality protein. Low-protein diets, such as MCD, have been used in the

past in mouse models to rapidly induce steatohepatitis and liver fibrosis. However, their current use is limited because they do not reproduce a realistic diet and the key metabolic alterations of human MASLD, particularly obesity and IR. Furthermore, mice fed MCD show marked weight loss, raising both scientific and ethical concerns. For this reason, MCD models may be more suitable in specific contexts, such as to study histological aspects of liver fibrosis and inflammation and test new targeted drugs, or to investigate altered drug disposition due to MASH-associated transporter alterations [30,37,38].

WD-fed mouse models are the ones that better recapitulate obesity, hypercholesterolemia, IR, and histological hallmarks of human disease progression and are best suited for testing therapies to promote weight loss and ameliorate inflammation [34,39]. Indeed, the range of WDs aims to mimic a high-fat/sugar, low-fiber intake. However, different sources of fat (e.g., lard, corn oil, milk) and carbohydrates (sucrose, fructose) can significantly influence MASLD outcomes [40,41]. WD regimens with varying macronutrient compositions and feeding durations induce a spectrum of alterations ranging from simple steatosis to MASH at 12–16, 20–24, and up to 9–18 months of age, depending on mouse genetics [33,42,43]. This diet triggers early and long-lasting alterations, including oxidative stress and mitochondrial dysfunction, hepatic iron deposition, and lipid peroxidation, as observed in the progression of MASLD in humans [43–46]. Notably, after WD feeding, different liver lobes in mice exhibit metabolic heterogeneity similar to humans: in 8-week-old C57BL/6J mice, the left lobe showed the earliest and most severe metabolic and inflammatory changes, which progressed further after 16 weeks [46]. Combining WD with drinking water supplemented with fructose, but not glucose and sucrose, exacerbated the progression of MASLD in male C57BL/6N mice after 10 weeks, as reported in humans consuming sugar-sweetened beverages [47,48]. However, the distinct effects of various types of sugars on the progression of MASLD are still a matter of debate. C57BL/6J mice were fed a WD containing ~30% fat and 20% sucrose supplemented with 30% fructose or sucrose in drinking water from 6 weeks of age for 24 weeks. A comparable progression of liver damage was observed regardless of the type of sugar addition [49]. WDs use in mice is translationally advantageous because with these diets, MASLD is not induced by nutritional deficiencies, unusual additives, hepatotoxins, or extremely high fat content (45–69%); therefore, they more closely resemble human dietary patterns and induce metabolic alterations that better recapitulate those observed in humans [34,39].

The Gubra Amylin (GAN) diet is attracting interest for its ability to induce MASLD, as its high fructose and saturated fat content mimics a typical "fast food" eating pattern [31]. This diet induced hepatic steatosis and mild inflammation in adult male C57BL/6J mice as early as 10 weeks of feeding, associated with colonic microbiota dysbiosis, an important cofactor in human MASLD [50]. However, the 2% cholesterol content of the GAN diet is substantially higher than that of standard Western diets (e.g., ~0.2% in WD) and therefore does not quantitatively reflect typical human dietary intake. Nevertheless, the clinical translatability of a C57BL/6J mouse model fed a diet with such a cholesterol concentration, with 40% of saturated fat (mainly palm oil) and 20% fructose for up to 44 weeks under normal housing conditions, was demonstrated [51–54]. Indeed, these mice showed clinical features, metabolic parameters, and histological alterations (macrovesicular steatosis, hepatocyte ballooning, inflammation, and fibrosis) consistent with human patients. These findings highlight their suitability for studying therapeutic targets for MASH, even with the disadvantage of long and expensive disease induction times. Interestingly, MASH and fibrosis can develop more rapidly and severely when this diet is fed to GEMs. Indeed, ob/ob mice fed GAN for 16 weeks rapidly developed steatosis, fibrotic MASH, lobular inflammation, hepatocyte ballooning, fibrotic liver lesions, and hepatic transcriptome changes [31].

The duration of the diet and the age at which it is started are further key factors: prolonged exposure to imbalanced diets induces the most severe alterations, closely resembling human disease, but at higher time and economic costs. In parallel, WD-fed mice display different severity of MASLD from preadolescence (20–30 days) or puberty (8 weeks) to mature adulthood (12 weeks), or until middle age (~15 months) and senescence (~20 months) [33,42,43,55,56]. Notably, the GAN diet seems to induce differential progression of MASH and fibrosis at different ages. 14-month-old C57BL/6J mice fed a GAN diet for 21 weeks developed severe pathological features of MASLD, comparable to those of humans, more rapidly than young mice [57]. Interestingly, in aged male mice, macrovesicular steatosis and hepatic immune cell infiltration (including monocyte-derived macrophages, Kupffer cells, and T cells) were already evident after 12 weeks of GAN feeding. In contrast, progression to MASH and fibrosis was observed in both aged male and female mice only after 21 weeks [57]. Furthermore, this mouse model developed HCC after approximately 60 weeks of feeding the GAN diet and was useful for testing lanifibranor and semaglutide, demonstrating the latter drug's ability to both improve advanced MASH and reduce cancer development [58].

Finally, the appropriate choice of a control diet is critical in study design to minimize experimental bias.

Interestingly, the AIN-93G diet, formulated to enhance growth and reproduction in mice [59], has been widely used in the past as a modified basis for high-calorie diets and HFDs, as well as for their comparison. However, this diet can induce weight gain and hepatic steatosis in C57BL/6J mice [60]. A healthy maintenance diet or a purified diet similar to the experimental one, except for the high-fat, sucrose, and cholesterol contents, could be successfully used as a control diet in mouse models [61].

2.2. Latest Research Moving Toward Combined Approaches and GEM Models of MASLD

The choice of the mouse strain is of great significance, leading to large differences based on the combination of dietary regimens and genetic background [62].

In particular, the choice of inbred animals raises additional concerns: their low genetic variability allows for more precise mapping of MASLD-related pathways and genes, but at the expense of representing human interindividual physiological diversity. Nevertheless, inbred mice are essential for creating and maintaining GEMs, and both strain and substrain significantly influence the MASLD phenotype and susceptibility to developing severe disease. Currently, several GEMs are available, including monogenic, polygenic, and liver-specific GEMs, with a well-established genetic background for metabolic studies and suitable for gene KO. Genetic alterations associated with fatty liver disease most commonly involve lipoprotein trafficking, glucose metabolism, adiposity/fat distribution, IR, or mitochondrial/endoplasmic reticulum biology.

GEMs represent valuable tools for studying MASLD, each of them having advantages and limitations. Monogenic mouse models offer insights into the role of specific genes and usually replicate the key human metabolic alterations, but may oversimplify the multifactorial nature of MASLD. Conversely, the strength of liver-specific genetic models lies in the study of specific molecular pathways without the confounding influence of metabolic comorbidities. However, these mouse models may present unexpected systemic alterations, which could interfere with the desired liver-specific phenotype, and also lack relevant interactions between the liver and adipose tissue, pancreas, and cardiovascular system. These mice may not be ideal for initial phenotyping of a novel gene's function, as the complex metabolic and interorgan crosstalk would be overlooked in a liver-specific mouse model. Conversely, a whole-organism KO mouse model could offer a broader view to study the physiological role of a gene, providing a systems perspective on metabolic

regulation that tissue-specific models may not capture. The choice of GEMs should therefore be carefully guided by the research question, balancing the goal of precise dissection of cell-specific mechanisms with the need to understand systemic complexity. Ideally, polygenic mouse models for MASLD would help improve the translation of preclinical findings into human clinical applications, but they are currently underutilized because they are more expensive and time-consuming than using established models [63].

Gene-environment interactions and health comorbidities have a significant role in MASLD susceptibility and severity in both humans and mice, with a particular focus on food composition [42,64]. For investigating these aspects, GEMs are often subjected to dietary interventions, which complement the study of metabolic dysfunctions and molecular mechanisms occurring at different stages of disease progression, such as oxidative stress and ferroptosis [34,44,63,65]. WDs appear to be the most widely administered dietary regimens to GEMs in recent research. However, one criticism of such diets is the lack of standardization. Variability in macronutrient and micronutrient content may contribute to differing results among murine studies and may hinder their translation into the clinical setting [66]. Furthermore, the sensitivity of different mouse models to husbandry conditions is often overlooked, depending on common practices and available laboratory resources. Interestingly, mouse housing temperature can impact liver disease modeling, and thermoneutrality (TN) conditions around 30 °C can exacerbate liver damage progression by influencing systemic metabolism through decreased thermogenesis and inflammation, compared to standard housing temperatures (20–24 °C) [33,34,62]. For instance, PWK/PhJ mice, fed WD and kept under TN conditions from 7 to 24 weeks of age, have been recently described as a promising mouse model with features of human MASH, showing more severe obesity and IR, higher liver enlargement, and serum levels of cholesterol and transaminases compared to other mouse strains, including C57BL/6J [62]. Notably, PWK/PhJ mice developed significant fibrosis and displayed distinct transcriptomic and mitochondrial alterations. Ten-week-old male C57BL/6J mice fed a similar WD for 13 weeks under TN showed more severe pathological, histological, and molecular features of MASLD than their counterparts raised at 22 °C [55].

In a comparative analysis of experimental conditions, TN impacted the development of MASLD mainly in the early stages of the disease rather than in the more advanced ones [60]. Diet composition played a key role in shaping MASLD at thermal neutrality, suggesting that TN rearing may reduce intragroup variability in response to WD feeding. Furthermore, a complex interaction between liver and adipose tissue was observed for the onset and progression of MASLD, depending on the housing temperature of the mice. In particular, an altered hepatic response to lipolysis of white adipose tissue and a reduced activation of brown adipose tissue in response to β3-adrenergic stimulation have been demonstrated [67]. However, TN did not clearly affect MASH progression towards fibrosis in 8-week-old male C57BL/6J mice compared to those maintained at standard room temperature after 4 and 7 months of GAN, showing a comparable histological pattern of liver disease [68].

Taken together, these findings suggest that careful consideration of TN could help optimize mouse models of MASLD by significantly reducing the dietary intervention time and the interindividual variability, which in turn increases the statistical power of the experiment, leading to a potential reduction in the number of animals needed to model MASLD. Despite this, its practical availability and management in laboratory animal facilities may vary [67].

Interestingly, most recent studies have been conducted in male mice, highlighting the need for future investigation on MASLD in females. This represents a limitation in current research and leaves a significant gender gap regarding the molecular mechanisms of MASLD. The protective role of estrogen in cardiovascular and metabolic diseases is

widely recognized, but in recent years, the health risks associated with MASLD in women have also become increasingly apparent [34,69,70]. Similar findings have been observed in female mice, which has led to the widespread and misleading use of male subjects to model MASLD, MASH, and fibrosis [71].

In this complex context, the ethical and practical aspects of experimental approaches to inducing MASLD in mouse models must also be considered. WD consumption for many weeks in wild-type mice or GEMs increases experimental costs and may lead to various adverse health conditions (reduced food intake, weight loss, microbiota dysbiosis, chronic joint pain, neurobehavioral alterations) likely related to the progression of liver injury and IR [42]. A high-fructose diet negatively impacts osteogenesis and bone density in mouse models, predisposing to osteoporotic fractures [35]. Raising mice in TN is controversial because it affects the animals' metabolism and immune function, which can potentially alter experimental results depending on the research context [33,34]. Consequently, increased suffering and mortality not only pose significant animal welfare concerns but also operational challenges, such as the need to use more animals to maintain statistical power in later phases of the study.

The multifactorial nature of the disease and the difficulty in selecting an appropriate MASLD murine model contribute to the incomplete understanding of its pathogenic mechanisms, particularly those leading from simple steatosis to steatohepatitis. The excess in dietary lipids and simple carbohydrates causes lipid droplet formation in hepatocytes, but these can be degraded to some extent by autophagy, preventing excessive tissue storage and subsequent cellular dysfunction. Thus, the role of autophagy in lipid homeostasis and its alteration in the development of MASLD has emerged. Regulatory changes in hepatocyte autophagy due to overnutrition and the influence of this process in other organs, such as adipose tissue, are under investigation.

New Zealand Obese (NZO) mice, a polygenic model of metabolic syndrome and type 2 diabetes, showed early obesity just at 22 weeks of age under a standard diet (SD), similarly to older 39-week-old C57BL/6J mice. Furthermore, they developed more pronounced MASLD when fed HFD (36% fat) for 16 weeks. The overall results were correlated with a decrease in hepatic autophagy [72].

Recently, a mouse model KO for mitogen-activated protein kinase 15 (*MAPK15*) on a C57BL/6J background has been characterized, highlighting a key role of this protein in the control of mammalian hepatic lipid homeostasis [73]. Specifically, wild-type and KO mice were fed a WD diet whose composition realistically mimicked the human imbalanced Western diet (38% fat, 0.2% cholesterol, 33% sucrose) from 8 to 24 weeks of age. The phenotypic, metabolic, and imaging characteristics of MASLD were monitored in vivo from early to later experimental stages. Interestingly, KO male mice developed earlier and more severe MASLD outcomes, including diet-induced obesity, increased blood transaminases, cholesterol, and glucose, and IR compared to their wild-type counterparts. Notably, male KO mice developed early liver changes on ultrasound, indicative of progressive worsening of hepatic steatosis, and some in the SD group showed mild hepatic steatosis. Histological analysis confirmed more severe hepatic steatosis and milder inflammation and fibrosis in male KO mice fed an HFD compared to controls. Consistent with the literature, KO female mice showed a milder phenotype than males, although a trend toward greater lipid accumulation in the liver compared to wild-type females was observed. Overall, these findings suggest that deletion of the *MAPK15* gene, under WD stimulation, worsens the progression of MASLD in mice. Importantly, transcriptomic analysis highlighted increased *MAPK15* expression in the liver of MASLD patients, suggesting a compensatory role in disease progression.

The role of adipose tissue-liver crosstalk in the pathogenesis of MASLD was specifically studied in young male C57BL/6J mice and in adipocyte-specific autophagy-related gene 7 (*Atg7*) KO mice fed a HFD (32% fat) for up to 8 months. No differences were evident between KO mice and controls under standard conditions, while HFD promoted autophagy in adipose tissue only in wild-type mice, worsening hepatic steatosis, inflammation, and fibrosis [74]. These observations suggest the potential of targeting autophagy in adipose tissue for MASLD/MASH treatment. However, these adipose-tissue-specific KO mice display hypertrophy of subcutaneous fat, but atrophy of visceral fat, while humans with MASLD typically show augmented visceral adiposity, which is strongly associated with metabolic dysfunctions and increased cardiovascular risk. This discordant pattern, which rather mimics human lipodystrophy, further highlights the need to carefully select mouse models based on specific research questions.

Another key mechanism leading to hepatic steatosis occurs when fatty acid uptake and synthesis exceed the capacity of hepatocytes to oxidize and export lipids. Recently, the role of A-kinase anchoring protein 1 (AKAP1) has been studied in *AKAP1*-deficient mice, both systemically and specifically in hepatocytes. This mitochondrial protein is involved in energy balance, regulation of lipid homeostasis, and MASLD. *AKAP1* KO diet-induced obesity mouse model on C57BL/6N background showed less severe weight gain and metabolic alterations, including hyperlipidemia and IR, as well as hepatic steatosis under HFD (60% fat) for 24 weeks, compared to wild type mice. Comparable results were reproduced in mice by treatment with AKAP1 inhibitors. Mechanistically, these findings were related to increased energy expenditure due to enhanced thermogenesis in brown fat via the activity of the mitochondrial enzyme acyl-CoA synthetase long-chain family member 1 (ACSL1). These findings were consistent with *AKAP1* downregulation found in subcutaneous adipose tissues of obese patients, compared to lean controls [75].

To analyze AKAP1 activity in hepatocytes, without the interference of increased energy expenditure in adipose tissue on fat accumulation in the liver, the same research group developed tissue-specific *AKAP1* KO mice on a C57BL/6J background. Liver- specific KO mice showed worsening hepatic steatosis and steatohepatitis under HFD (60% fat) or WD (40% fat, 0.2% cholesterol) combined with 45% glucose and 55% fructose in drinking water up to 24 weeks. Conversely, restoring hepatic *AKAP1* by knocking down Glycerol-3-phosphate acyltransferase 1 (*GPAT1*) improved the disease [76]. Interestingly, the moderate-fat, moderate-cholesterol diet supplemented with complex sugars induced human-like histological features of MASH in this mouse model as early as week 16, including hepatocyte ballooning and fibrosis associated with obesity, dyslipidemia, and IR. Mechanistically, AKAP1 can inhibit triglyceride synthesis in hepatocytes by phosphorylating and inactivating GPAT1, a mitochondrial outer membrane protein that converts acyl-CoAs to lysophosphatidic acid. This finding would be consistent with the clinical literature, which describes a loss-of-function *GPAT1* genetic variant with a protective role against MASLD, while a gain-of-function mutation increases predisposition to the disease. Thus, this mouse model revealed that *AKAP1* deficiency would predispose to hepatic steatosis mainly through positive regulation of triglyceride synthesis via enhanced mitochondrial GPAT activity, which appears as a novel potential therapeutic target.

Recently, young mice carrying the Ay (Agouti Yellow) mutation on a C57BL/6J background have been used to study MASLD. Mice were fed a diet high in fat (42%), cholesterol (0.2%), and sucrose (24%), and drinking water sweetened with fructose (23 g/L) and glucose (19 g/L). After 16 weeks, they developed hyperphagia, obesity, hypertriglyceridemia, IR, and hepatic steatosis, including inflammation and fibrosis, progressing to more advanced lesions after 12 months [53]. Interestingly, 8-week-old male and female C57BL/6J mice fed a comparable diet until 6 months of age showed increased food intake, weight

gain, liver-to-body weight ratio, transaminases, blood glucose, insulin levels, and total cholesterol compared to controls, as well as steatosis and hepatocellular ballooning, but not inflammation and fibrosis [69]. Consistent with the literature, female mice showed less severe metabolic alterations and hepatic steatosis than males. Concordant metabolic and histological findings were highlighted in C57BL/6J mice of both sexes fed a high-cholesterol, high-sucrose diet (38% fat; 47% carbohydrate, 33% sucrose) with a comparable experimental design [77]. Overall, these models resemble MASLD induced by a fast food-like diet and could be useful for studying its pathogenesis and developing preventive or therapeutic treatments.

Although generally associated with overweight or obesity, MASLD is increasingly being diagnosed in lean people as well, associated with a significant cardiovascular risk. Lean-MASLD mouse models, such as *Lrpprc* KO mice, are therefore attracting attention, as they display sex-dependent cardiometabolic alterations triggered by impaired mitochondrial integrity and β-oxidation [78].

Recently, the role of the gut-liver axis has also been highlighted. Studies conducted in KO mice for *Tm6sf2*, a regulator of hepatic lipid metabolism expressed in liver and small intestine, have shown that intestinal *Tm6sf2* deficiency primarily promotes MASH in both male and female mice, further worsening on CD or WD. Indeed, *Tm6sf2* deficiency impairs intestinal barrier function, promoting the translocation of free fatty acids, endotoxins, and other harmful metabolites into the circulation and subsequently to the liver, thereby inducing steatosis and inflammation. These effects are further amplified when combined with CD or WD feeding [79].

Lately, polygenic models of obesity are emerging as new models of diet-induced MASLD. For instance, TALLYHO/JngJ and NONcNZO10/LtJ mouse strains, with a genetic predisposition to overweight while on an SD, were fed an HFD containing 1% of cholesterol and supplemented with fructose/sucrose (55/45%) in drinking water for 16 weeks [63]. Comparative pathology analysis showed that these mouse models developed metabolic and histological alterations, including hepatocyte ballooning and steatosis, as well as mild inflammation and fibrosis comparable to the spectrum observed in early human MASH. Furthermore, TALLYHO/JngJ mice developed signs of kidney damage similar to those of patients with cardiorenal syndrome. Interestingly, these models were useful in demonstrating the ability of empagliflozin, a sodium-glucose cotransporter 2 inhibitor, to significantly attenuate the histological outcomes of MASLD [63].

Lipid-induced oxidative DNA damage in hepatocytes is strongly suspected to induce carcinogenesis. Therefore, efforts are intensifying to develop mouse models that mimic the evolution of MASH and fibrosis in HCC, particularly GEMs or specific mouse strains. Eight-week-old C57BL/6NJ mice, fed WD (42% kcal from fat, 0.2% cholesterol, 42.7% carbohydrate) and drinking water supplemented with 2% fructose and glucose for up to 54 weeks, developed hepatocellular ballooning, inflammation, and fibrosis as early as 16 weeks. Progressive worsening was observed beyond 32 weeks, as well as spontaneous HCC [51].

Notably, this substrain differs from the parental C57BL/6J by having a functional *Nnt* gene and shows enhanced impairment of glucose metabolism but similar susceptibility to metabolic diseases when on a high-fat/high-sucrose diet [80].

A similar 36-week dietary intervention induced higher levels of transaminases and plasma cholesterol, as well as greater liver inflammation, fibrosis, and HCC incidence in adult *Cyp2a12/Cyp2c70* knock-out (DKO) male mice compared to WT mice [81]. Considering interspecies differences, this DKO GEM lacks two enzymes responsible for increased bile acid hydrophilicity in mice, thus presenting a bile acid composition like that of humans. Therefore, evidence from this model suggests that accumulation of hydrophobic bile acids

in the liver is a key mechanism promoting MASH/HCC progression and thus a potential preventive and therapeutic target.

Overall, recent research emphasizes that careful selection of diet, mouse strain, study duration, use of GEMs, and housing conditions is critical in modeling MASLD (Table 1). The complex interactions among genetic, dietary, and environmental factors remain a significant challenge, and polygenic models may help to overcome these limitations. Furthermore, liver-humanized mice may be particularly valuable to study metabolism and the effect of therapeutic molecules, because they closely replicate enzymatic features of human hepatocytes, while their use to study metabolic disorders is currently controversial [28].

Table 1. Current evidence from mouse models of MASLD and comparative pathological features relevant for clinical translation.

Experimental Setup				Key Phenotypes for MASLD Comparative Pathology		Ref.
Genotype	**Sex**	**Diet and Inducing Cofactors**	**Age/Timing of MASLD Induction**	**Metabolic**	**Histologic**	
C57BL/6J	Male	CD	10-weeks-old/ 20 weeks	Hepatomegaly ↓ BW ↓ plasmatic transaminases, insulin and glucose	Steatosis Inflammation Fibrosis HCC	[39]
C57BL/6J	Male	HFD	4-weeks-old/ 17 months	Hepatomegaly ↑ BW ↑ IR Transcriptome changes in collagen and lipid regulatory genes	Steatosis	[42]
NZO (C57BL/6J background)	Male	HFD	7 weeks-old/ 32 weeks	Hepatomegaly ↑ BW ↑ autophagy-related proteins	Steatosis	[72]
C57BL/6J	Male and female	WD	8-weeks-old/ 17 weeks	Hepatomegaly ↑ BW Sexual dimorphism ↑ plasmatic transaminases, cholesterol, insulin and glucose In vivo heart, kidney, liver US alterations Kidney alterations	Steatosis	[77]
C57BL/6J	Male	WD	8-weeks-old/ 16 weeks	Changes in lipidome and metabolome profiles comparable to those in humans		[46]
C57BL/6N	Male	WD + fructose	8-weeks-old/ 10 weeks	Hepatomegaly ↑ BW IR ↑ plasmatic transaminases, cholesterol, insulin and glucose autophagy-related transcriptome changes	Steatosis	[57]

Table 1. *Cont.*

Experimental Setup				Key Phenotypes for MASLD Comparative Pathology		Ref.
C57BL/6J	Male	WD + fructose/glucose	6 weeks-old/ 24 weeks	Hepatomegaly ↑ BW IR ↑ plasmatic transaminases, cholesterol, insulin and glucose ↑ lipogenic enzymes ↑ oxidative stress markers ↑ lipid peroxidation	Steatosis Inflammation Fibrosis	[49]
C57BL/6J	Male	WD + fructose/glucose	8 weeks-old/ 25 weeks	Hepatomegaly ↑ BW IR ↑ plasmatic transaminases, cholesterol, insulin and glucose	Steatosis	[52]
C57BL/6J	Male	WD + TN	10-weeks-old/ 13 weeks	Hepatomegaly ↑ BW IR ↑ plasmatic insulin and glucose Transcriptome changes in response to β3-adrenergic stimulation	Steatosis Inflammation Fibrosis	[67]
C57BL/6J	Male	GAN + TN	8 weeks-old/ 7 months	↑ BW ↑ plasmatic transaminases	Steatosis Inflammation	[68]
C57BL/6J	Male	GAN	8 weeks-old/ 44 weeks	Hepatomegaly ↑ BW IR ↑ plasmatic transaminases, cholesterol, insulin and glucose MASH-related transcriptomic alterations	Steatosis Inflammation Fibrosis	[54]
C57BL/6J	Male	GAN	6 weeks-old/ 10 weeks	Hepatomegaly ↑ BW ↑ plasmatic cholesterol Microbiota alterations	Steatosis Mild inflammation	[50]
C57BL/6J	Male and female	GAN	14 months-old/ 10 weeks	Hepatomegaly ↑ BW Sexual dimorphism Hepatomegaly ↑ plasmatic transaminases, cholesterol, insulin and glucose	Accelerated steatosis and inflammation	[57]
C57BL/6J	Male	GAN	6 weeks-old/ 72 weeks	Hepatomegaly ↑ BW ↑ plasmatic transaminases ↑ fibrosis markers	Steatosis Inflammation Fibrosis HCC	[58]
C57BL/6NJ	Male	WD + fructose/glucose	8 weeks-old/ 54 weeks	Hepatomegaly ↑ BW ↑ plasmatic transaminases, cholesterol, insulin and glucose	Steatosis Inflammation Fibrosis HCC	[51]

Table 1. *Cont.*

Experimental Setup				Key Phenotypes for MASLD Comparative Pathology		Ref.
PWK/PhJ (C57BL/6J background)	Male	WD + TN	7 weeks-old/ 18 weeks	Hepatomegaly ↑ BW IR ↑ plasmatic transaminases, cholesterol, insulin and glucose Transcriptomic and mitochondrial alterations	Steatosis Inflammation Fibrosis	[62]
AKAP1 KO (C57BL/6N background)	Male	HFD	8-weeks-old/ 24 weeks	↓ BW Hyperlipidemia ↑ thermogenesis	Steatosis	[75]
Liver specific-*AKAP1* KO (C57BL/6J background)	Male	HFD/ WD + fructose/ glucose	8-weeks-old/ 24 weeks	Hepatomegaly ↑ BW IR ↑ plasma lipids ↑ mitochondrial GPAT activity	Steatosis Inflammation Fibrosis	[76]
Atg7 KO (C57BL/6J background)	Male	HFD	8 weeks-old/ 8 months	Hepatomegaly ↓ BW ↑ plasmatic transaminases ↓ expression of autophagy-related proteins	Steatosis Inflammation Fibrosis	[74]
MAPK15 KO (C57BL/6J background)	Male and female	WD	8-weeks-old/ 17 weeks	Hepatomegaly ↑ BW Sexual dimorphism ↑ plasmatic transaminases ↑ cholesterol ↑ insulin and glucose in vivo US alterations	Steatosis Mild inflammation Fibrosis	[73]
Ay (C57BL/6J background)	Male	WD + fructose/glucose	8-weeks-old/ 12 months	Hepatomegaly ↑ BW IR ↑ plasma lipids	Steatosis Inflammation Fibrosis	[53]
Liver specific-*Lrpprc* KO (C57BL/6N background)	Male and female	SD	8-weeks-old/ 14 weeks	↓ Liver weight ↓ BW Sexual dimorphism ↓ weight heart, adipose tissue, soleus ↓ insulin and glucose ↑ plasma lipids Cardiometabolic impairment Mitochondrial disfunction ↑ ER stress markers	Steatosis Inflammation Fibrosis	[78]
Intestine-specific *Tm6sf2* KO (C57BL/6 background)	Male	CD/WD	7 weeks-old/ 8/14 weeks	Hepatomegaly ↑ BW ↑ plasmatic transaminases ↑ cholesterol Microbiota alterations	Steatosis Mild inflammation	[79]
TALLYHO/JngJ and NONc-NZO10/LtJ	Female	HFD + fructose/glucose	4 weeks-old/ 16 weeks	Hepatomegaly ↑ BW IR ↑ plasmatic transaminases ↑ cholesterol ↑ insulin and glucose Kidney injury	Steatosis Inflammation Fibrosis Ballooning	[63]

Table 1. *Cont.*

Experimental Setup				Key Phenotypes for MASLD Comparative Pathology		Ref.
Cyp2a12/Cyp2c70 KO (C57BL/6J background)	Male	WD + fructose/glucose	11 weeks-old/36 weeks	Hepatomegaly ↑ BW ↑ plasmatic transaminases ↑ cholesterol ↑ insulin and glucose	Steatosis Inflammation Fibrosis HCC	[81]

Abbreviations: BW, body weight; CD, choline-deficient diet; ER, endoplasmic reticulum; GAN, Gubra Amylin diet; HCC, hepatocarcinoma; HFD, high-fat diet; IR, insulin resistance; SD, standard diet; TN, thermoneutrality; WD, western diet. Symbols: ↑, increase; ↓, decrease; +, plus.

3. Histopathological Findings in MASLD

From a histopathological perspective, MASLD in humans is characterized by a set of hallmark features, including steatosis—defined as fat accumulation in more than 5% of hepatocytes and often predominantly localized in zone 3—together with inflammation, hepatocellular ballooning, and variable degrees of fibrosis. As the disease progresses, MASLD may evolve into MASH, which is distinguished by more pronounced inflammation and ballooning and may ultimately progress to cirrhosis. Typical liver histological findings include lipid droplets, inflammatory infiltrates composed of macrophages, neutrophils, and lymphocytes, ballooned hepatocytes (enlarged and injured cells), Mallory–Denk bodies, and perivenular fibrosis [82–84], which can also be exacerbated by the activation of hepatic stellate cells (HSC) [85]. Indeed, HSC can transdifferentiate into fibrogenic myofibroblasts, playing a critical role in the progression of MASLD into MASH and cirrhosis [85].

In murine models of MASLD, research efforts are therefore focused on recapitulating the key histopathological features observed in human disease. As reviewed by Vacca et al. [34], no single model currently reproduces all the phenotypic and histological characteristics of human MASLD. Some models effectively simulate the metabolic aspects of the disease but exhibit a milder histological phenotype, whereas others rapidly progress to MASH with significant fibrosis. Nevertheless, several key histologic features of MASLD can still be observed in the livers of these models. These include the presence of both microvesicular and macrovesicular steatosis with lipid droplets of varying sizes, hepatocellular ballooning (Figure 2), and, in more severe models, the development of fibrosis. The identification of macrovesicular versus microvesicular steatosis represents a key aspect of the histological assessment of MASLD. These two patterns can be distinguished based on the morphology and positioning of the hepatocyte nucleus. In hepatocytes with macrovesicular steatosis, a large central lipid droplet displaces the nucleus toward the cell periphery, frequently causing nuclear distortion and increased elliptical eccentricity. In contrast, in microvesicular steatosis, the nucleus generally remains centrally located and retains a more rounded morphology, as it is surrounded by multiple small lipid droplets [86].

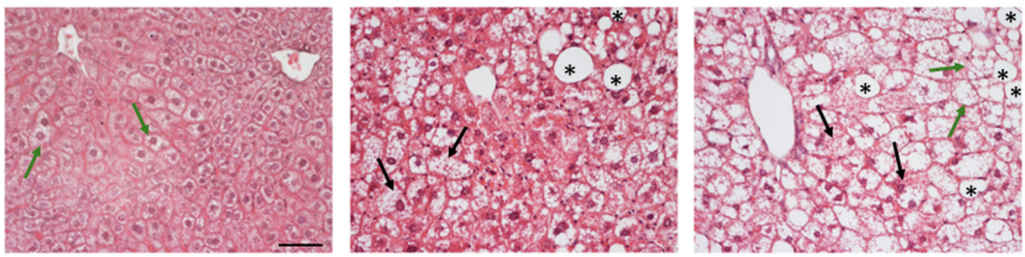

Figure 2. Representative H&E-stained images of murine liver sections illustrating different types of liver damage: macrovesicular steatosis (asterisks), microvesicular steatosis (green arrows), and hepatocellular ballooning (black arrows). Scale bar 50 µm.

Importantly, microvesicular steatosis is often associated with a more severe clinical and pathological context. It has been linked to increased inflammation, oxidative stress, and mitochondrial dysfunction [87]. Histological analyses indicate that approximately 10% of patients with NAFLD/MASLD exhibit microvesicular steatosis, which correlates with hepatocellular ballooning, mitochondrial abnormalities, and more advanced fibrosis [88]. Despite this, the mechanism underlying the development and progression of microvesicular steatosis, as well as the precise role of dietary factors in driving this phenotype, remains largely underexplored in both humans and murine models, with only a few papers reporting the occurrence of diet-induced microvesicular steatosis in models exposed to WD [89].

In both human and murine studies, histological staining techniques such as hematoxylin and eosin (H&E), Oil Red O, and Masson's trichrome or Sirius red are commonly employed to visualize, respectively, overall liver architecture, lipid accumulation, and the presence and extent of fibrosis, thereby enabling the systematic assessment and scoring of histopathological features according to the established scoring systems [83,90,91].

The first histological scoring system in humans in the liver field was the METAVIR (initially used for hepatitis C and subsequently validated for almost all chronic liver diseases), which evaluates viral activity and classifies fibrosis into 4 states based on its extent [92]. Subsequently, in 2002, the National Institute of Diabetes, Kidney, and Digestive Diseases validated the NAS (NAFLD Activity Score) histological scoring system [93], which provides a semiquantitative assessment of steatosis (0–3), lobular inflammation (0–3), hepatocellular ballooning (0–2), and fibrosis (0–4). There are also other scoring systems, such as those by Brunt and Goodman, which differ slightly from NAS and incorporate the evaluation of portal inflammation, and more recently, the Fatty Liver Inhibition of Progression Pathology Consortium developed the SAF score algorithm (Steatosis, Activity and Fibrosis), which is able to distinguish between steatosis and necroinflammation [93–96]. Usually, based on the NAS score, the pattern of liver injury, and the presence and severity of individual lesions, human biopsies can be classified as MASLD (not MASH), borderline MASH with a zone 1 pattern, borderline MASH with a zone 3 pattern, or definite MASH. Liang et al. [97] showed that NAS is also highly reproducible across rodent models, and nowadays it remains widely used for evaluating MASLD in mice, although, from a histological perspective, mice exhibit different liver patterns compared to humans (Table 2).

Table 2. Histopathological differences between human and mouse liver in MASLD.

Histological Feature	Human MASLD/MASH	Murine MASLD/MASH Models	Ref.
Steatosis	Diffuse macrovesicular steatosis, often centrilobular	Model dependent, sometimes prevalently microvesicular or patchy	[82–84,98]
Hepatocyte ballooning	Common in MASH	Often less pronounced than in humans	[63,82–84]
Lobular inflammation	Disseminated inflammatory infiltrates, mainly mononuclear cells	Milder inflammatory infiltrates; certain models show a predominance of intrahepatic T cells	[63,82–84]
Perisinusoidal/ pericellular fibrosis	Progression to pericellular and periportal fibrosis in advanced MASH	Variable, some models display mild to moderate fibrosis with slow and less severe progression; others display rapid progression	[38,57,63,82–84]

Table 2. *Cont.*

Histological Feature	Human MASLD/MASH	Murine MASLD/MASH Models	Ref.
Hepatic stellate cell (HSC) activation	HSC could have a role in exacerbating MASLD into MASH and inducing fibrosis	HSC activation occurs in response to injury, but with variable kinetics	[85,99–101]
Lobular zonation	Disease initially affects zone 3 and then spreads	Segmental or lobar heterogeneity	[46,82]

In mice, liver evaluation is typically performed after euthanasia, allowing collection of the entire organ and enabling accurate and comprehensive histological assessment and scoring. In human MASLD, biopsy is usually not recommended by guidelines as a first-line tool for screening, but it becomes necessary when non-invasive tests (NITs) provide discordant data or when alternative aetiologies of liver disease are suspected. Indeed, thanks to this technique, it is possible to detect microscopic abnormalities and quantify the degree of liver inflammation associated with liver damage, together with the evaluation of the extent of fibrosis [102]. In this context, the most commonly used techniques in clinical practice are percutaneous and transvenous biopsies. The choice between these approaches is guided by individual patient characteristics, including the presence of ascites, BMI, coagulation disorders, thrombocythemia, and the need for concurrent hemodynamic evaluation or measurement of the hepatic venous pressure gradient. Percutaneous biopsy is performed in the supine position, and the localization of the liver between the sixth and ninth ribs is performed by percussion or with an ultrasound (US), Computed Tomography (CT), or Magnetic Resonance Imaging (MRI) guidance. In this case, it is essential to obtain a sample of intact liver tissue of an adequate size that allows observation of globular structures and portal tracts (at least 11 portal tracts obtainable using a 16-gauge needle) [103].

Given the bleeding risk associated with percutaneous biopsy, transvenous biopsy is recommended in patients with ascites or coagulopathy. The patient is sedated, and the procedure is performed under real-time fluoroscopic guidance and continuous cardiac monitoring to detect potential ventricular arrhythmias caused by catheter passage through the right atrium. In this case, the preferred approach is via the right internal jugular vein, which is catheterized under US guidance and local anesthesia, with the patient in the supine position and the head rotated to expose the access site. From there, the guidewire reaches the inferior vena cava and advances to the right hepatic vein. A liver sample is obtained using an 18–19-gauge biopsy needle and must be at least 15 mm in length to be adequate for histological analysis.

Another commonly used approach is the transfemoral route, which offers the advantage of allowing measurement of the hepatic venous pressure gradient (HVPG), useful for assessing portal hypertension. A significant increase in HVPG is indeed an important indicator of liver failure in patients with MASLD [104].

Another valid alternative is represented by laparoscopic biopsy, a technique that allows direct visualization of the liver parenchyma and immediate intervention with electrocauterization in the event of bleeding. Currently, biopsies can also be performed using mini laparoscopy, which employs optical systems and instruments smaller than 2 mm. These are introduced through a peri-umbilical incision and advanced to the liver parenchyma after the creation of a pneumoperitoneum [21].

One last important technique is endoscopic ultrasound–guided liver biopsy (EUS-LB), which is performed using an EUS echoendoscope capable of acquiring both ultrasound and Doppler images for accurate visualization of vascular and anatomical structures. Tissue samples are typically obtained using a 19-gauge Tru-Cut needle, 19-gauge flexible fine-

needle aspiration (FNA) needles, or fine-needle biopsy (FNB) needles. Compared with Tru-Cut and FNA needles, FNB needles allow the acquisition of liver tissue specimens that are more suitable for histological analysis [105].

All these biopsy techniques can lead to both major and minor complications, the most common of which include bleeding (intra-abdominal or intrahepatic bleeding occurs in approximately 10% of percutaneous or transvenous biopsies, although severe bleeding is reported in only about 2% of cases), pain (reported in 30–50% of patients), and infection. Mortality is estimated at less than 1 case per 1000 procedures. Other potential complications include injury to adjacent organs and specific complications related to trans-jugular access, such as arrhythmias, neck hematoma, pneumothorax, transient Horner's syndrome, and arteriovenous fistula [103,106,107].

Considering these implications, in recent years, increasing efforts have been made to utilize data derived from liver biopsies to develop more innovative diagnostic approaches, including metabolomics-based methods and neural network–based models that integrate multiple histological features. In parallel, there is growing interest in the development of NITs, ranging from serological markers to various imaging techniques. These approaches may enable longitudinal monitoring and follow-up of the disease in a less burdensome manner for patients, while addressing key limitations of conventional histological scoring systems—such as the substantial time required for evaluation by experienced pathologists and the susceptibility to inter- and intra-observer variability [108–110]. For example, machine learning techniques can identify histological features that may escape the human eye, helping to predict disease progression and identify patients at risk of severe outcomes [111]. Besides, some Artificial Intelligence (AI) systems have been introduced: GENESIS and qFIBS use AI together with second harmonic fluorescence/two proton excitation techniques to quantify fibrosis, ballooning, steatosis, and inflammation in patients with MASH [112].

In this context, focusing on the translational potential of imaging techniques from murine models to humans and the identification of shared biomarkers may be highly relevant for the development of future approaches to MASLD.

4. MASLD: Clinical and Experimental Imaging Assessment

4.1. Emerging Role of MASLD Imaging in Clinical Practice and Preclinical Research

The use of imaging techniques for the diagnosis and monitoring of MASLD in humans is currently growing and now represents a fundamental complement to liver histology. Advanced imaging techniques are increasingly recommended by clinical guidelines for the effective management of MASLD, playing a crucial role in large-scale screening of high-risk populations, disease follow-up, and assessment of patient response to treatment [113].

Histopathological analysis remains essential for definitive confirmation and staging of MASLD, and clinical guidelines suggest its opportunity, especially in patients with MASLD who are at increased risk of steatohepatitis and advanced fibrosis [114].

Nonetheless, imaging techniques help overcome its limitations by allowing real-time longitudinal examination of the entire organ and facilitating the study of pathological alterations with heterogeneous distribution. Imaging techniques can be useful both in the diagnosis and in assessing the severity of fatty liver disease. Additionally, imaging can guide liver biopsies, minimizing the risks associated with traditional invasive practices, which can be reserved for cases where NITs are not fully informative [115]. Overall, the importance of investigating MASLD using non-invasive diagnostic methods and integrated, multiparametric approaches, including biochemical markers, omics data, and imaging techniques, is now recognized.

The use of imaging methods for MASLD is rapidly expanding from humans to murine models. This shift is driven by the need for non-invasive, longitudinal monitoring of

disease progression, capturing the dynamics of the disease. The integration of imaging into preclinical studies allows for better translation of experimental findings into clinical trials, aiding the development of therapies for MASLD/MASH.

Monitoring animals with these techniques allows repeated longitudinal monitoring of the same animal and statistically minimizes inter-individual variability because each subject serves as its own control. The World Federation for Ultrasound in Medicine and Biology (WFUMB) guidelines recommend liver biopsy and magnetic resonance imaging proton density fat fraction (MRI-PDFF) as reference methods for the diagnosis of MASLD. However, their limitations (e.g., invasiveness, relatively high cost, availability, and patient compliance) may be overcome by newer, less invasive, and more accessible US-based software tools for liver fat quantification [116]. These advanced, quantitative imaging techniques provide an objective measurement of liver fat content, which can be compared over time and correlates well with liver triglyceride content, complementing histological findings.

Among the wide range of imaging modalities, US Share Wave Elastography, MRI, and chemical shift–based water–fat separation techniques, such as magnetic resonance spectroscopy (MRS), have been employed [112]. In both species, these techniques enable non-invasive assessment of hepatic steatosis, liver morphology, and disease progression, supporting longitudinal studies. The translational value of US and MRI between mice and humans depends heavily on intrinsic differences in anatomy, physiology, and technical requirements for imaging such small animals, as well as differences in perspective and resources. Despite the advantages, the translational gap in imaging studies between mice and humans arises from the need for much higher imaging resolution in mice, different clinical and experimental objectives, and logistical and ethical constraints. None of the currently available imaging methods is able to assess the relevant microscopic features of MASLD as well as histological examination. However, better matching between clinical and preclinical imaging protocols could improve the translational potential of mouse models.

4.2. Updates in Comparative Liver US

US is the most practical, safe, and cost-effective imaging technique for monitoring hepatic steatosis in both clinical and experimental settings.

Qualitative assessment of liver echotexture changes, increased echogenicity, and US attenuation are useful features of hepatic steatosis in humans and mice, which hinder clear visualization of the diaphragm, bile ducts, intrahepatic arteries, and the deeper portion of the liver.

While semi-quantitative scores can be derived from these US characteristics, such as comparing liver echogenicity to that of surrounding organs like the kidneys, their accuracy depends largely on the experience of the sonographer, the standardization of evaluation criteria, and the performance of the equipment [116–118]. On the other hand, this scientific concern is comparable to that related to the wide inter-observer variability in the interpretation of the histological classification of steatosis, promoting the adoption of digital pathology and AI in this field as well [119]. Therefore, a shift from qualitative, semiquantitative B-mode imaging towards quantitative ultrasound (QUS) techniques has provided more objective, reproducible, and accurate measurements of liver fat content.

QUS analysis of hepatic steatosis in humans appears reproducible to screen MASLD [120], showing good sensitivity and specificity (about 90%) for the detection of moderate and severe hepatic steatosis, while the ability to detect mild and diffuse liver disease is limited [121–123].

Until recent years, the hepatorenal index (HRI) has been an easy-to-use, semi-quantitative US parameter to assess mild to severe hepatic steatosis in patients, based on the ratio between the echogenicity of the liver parenchyma and that of the right renal cortex [124]. HRI is a more objective, operator-independent method compared to subjective

visual assessment, and its reproducibility has been further improved by AI [125]. However, concerns about renal cortex backscatter anisotropy or assumptions about renal health status have led to criticism of its accuracy [121,126].

QUS enables non-invasive assessment of hepatic steatosis, fibrosis, and inflammation in MASLD. Current WFUMB's recommendations highlight the usefulness of the most recent advancements in QUS imaging, including Attenuation Imaging (ATI), backscattered coefficient (BSC), or speed-of-sound (SoS) algorithms for quantifying liver fat content, as well as their current limits in protocols standardization and confounding factors like high BMI [121]. Of note, multiparametric analysis shows promise to improve QUS accuracy, but further evaluation is needed before its routine implementation in clinical practice [127].

Other advanced QUS techniques, such as shear wave elastography (SWE), strain-based real-time elastography (RTE), and shear wave dispersion (SWD), can be combined with ATI for simultaneous assessment of lipid content, stiffness, and viscoelastic properties of liver tissue, respectively. These features are related to hepatic steatosis, fibrosis, and inflammation, which are key histological features in MASLD [128]. Interestingly, hybrid thermoacoustic imaging has recently demonstrated the potential to accurately measure liver fat fraction, overcoming the limitations of current QUS methods in obese patients, in line with reference MRI-PDFF techniques.

Efforts are underway to translate comparable QUS approaches into mouse models of MASLD. However, there are technical challenges related to the need for high-frequency probes and specialized hardware to achieve the necessary resolution due to their small size.

In particular, practical limitations such as proprietary software, sophisticated equipment, and time-consuming specialized skills limit the widespread use of advanced techniques such as ATI and SWE compared to other QUS techniques.

Furthermore, the mouse liver is accessible through a small acoustic window, making it difficult to measure liver stiffness, and anesthesia is required to control motion artifacts. Notably, the characteristics of liver parenchymal structure differ between humans and mice, as well as during MASLD progression, and US scattering and attenuation properties of tissues are frequency-dependent, influencing the interspecific attenuation and stiffness threshold values.

Despite these challenges, preclinical studies have demonstrated that the use of high-frequency, dedicated systems and multiparametric approaches, including computer-aided analysis of B-mode images, offers a powerful tool to enhance preclinical MASLD research in line with the 3Rs principles (replacement, reduction, refinement) [129].

The most technologically advanced US-based methods recently applied to mouse models include US-induced thermal strain imaging, US molecular imaging using targeted microbubbles for disease markers, and SWE [129–131]. Previous efforts to characterize hepatic steatosis by texture analysis on ex vivo C57BL/6 and ob/ob mice US images, and recently on living C57BL/6J mice and *MAPK15* KO mice, have demonstrated that complementary approaches, including semi-quantitative and parametric US data, are feasible and useful for the practical detection of longitudinal MASLD-related changes of the murine liver, with efficient processing times and good concordance with histology [22,132]. Recently, AI applications to preclinical imaging have been stimulated to improve the extraction of complex disease-related patterns, also from US images [133]. Furthermore, a novel multifrequency US technique, which uses a narrow bandwidth to achieve a higher sound-to-noise ratio and thus improve QUS measurements, has been preliminarily tested in murine models of MASLD, showing promising results for liver tissue characterization and potential clinical applications [134].

4.3. Recent Advances in Translational MRI

Currently, QUS represents an accessible first-line option for routine patient screening and monitoring, and improvements in US-based attenuation measurement have led to good concordance with MRI-PDFF [135]. However, MRI-based methods, including PDFF and chemical shift MRI, offer greater diagnostic accuracy for detecting and grading liver steatosis [116].

Nonetheless, MRI-PDFF has limitations in patients with metallic implants and shows relatively longer acquisition times than QUS, as well as logistical constraints for patients with reduced mobility, which can be partially overcome by using low-magnetic-field MRI scanners [136]. Therefore, these techniques can be used in a complementary way to balance different clinical needs.

Emerging evidence supports the use of MRI-PDFF for the reproducible measurement of liver fat content, which is considered the non-invasive reference method for monitoring liver steatosis progression and treatment response in clinical trials [137].

Specifically, MRI-PDFF and histological examination use different approaches to measure hepatic steatosis: the former measures fat signals, while the latter evaluates the morphology and distribution of affected hepatocytes. Notably, a clinical study investigating the diagnostic performance of liver MRI-PDFF for fat quantification demonstrated good concordance with liver biopsy, also in obese patients [138].

Iron stores, fibrosis, and liver function can be accurately assessed in a multiparametric way by transverse relaxation rate (R2*) measurement, MR elastography, and hepatobiliary phase MRI, respectively [137,139]. Additionally, a recent feasibility study demonstrated the potential for non-invasive assessment of liver inflammation using diffusion-based magnetic resonance imaging (dMRI) cytometry. This method was able to assess liver microstructure, including cell size and density, and histology-based simulations confirmed imaging findings [140]. Similar to QUS, AI algorithms may further improve the performance of MRI in the management of MASLD, but liver biopsy remains the most sensitive test for early stages of steatosis and fibrosis [141].

Multiparametric quantitative MRI has emerged as a powerful, non-invasive tool for diagnosis and disease monitoring in preclinical mouse models, closely mimicking human imaging protocols, including MRS, Dixon-based, and dynamic contrast-enhanced (DCE) sequences.

These techniques provide high-resolution, whole-organ assessment of liver pathology, including hepatic steatosis, MASH, fibrosis, and iron overload, showing strong correlations with destructive techniques such as histology and liver lipid extraction [142–144]. Of note, preclinical application of MRI is technically challenging due to the need for high field strengths to achieve adequate spatial resolution, interference from motion artifacts, and the small size of the target organ. In particular, scanners with magnetic field strengths above 3 Tesla, commonly used in mouse models, proportionally increase phase errors and magnetic field inhomogeneities, hindering the separation of fat and water signals and the accuracy of the PDFF. Despite these challenges, advanced MRI in mouse models of MASLD proves useful for gaining a deeper understanding of pathogenic mechanisms and identifying new therapeutic targets, as well as for validating new diagnostic approaches or testing new drugs.

MRS has been used in vivo in CD-fed C57BL/6 male mice to longitudinally characterize changes in intrahepatic fatty acid and/or collagen composition from the early stage of MASLD to the more advanced stages of fibrosis-associated MASH. High resolution 9.4 T magnet and specialized sequences, such as stimulated echo acquisition mode (STEAM) combined with water suppression-variable pulse powers and optimized relaxation delays

(VAPOR) algorithms or DCE imaging using gadolinium-hydrazide, showed a good concordance with gas chromatography-mass spectrometry (GC–MS) and histology [143,145].

These studies could provide new translational information for non-invasive risk stratification in patients, highlighting the relevance of monitoring lipid or collagen composition, in addition to total fat.

In the same mouse model, high-field MRI was used to evaluate the efficacy of antifibrotic treatment with the polyethylene glycol fibroblast growth factor 21 (PEG-FGF21v) variant on liver steatosis and fibrosis, with clear correlations with histology, potentially guiding future translatable studies [146]. Similarly, HFD-fed C57BL/6J male mice treated with a glucagon-like peptide-1 receptor and glucagon receptor dual agonist were monitored via a 9.4 T scanner using proton density and R2* values to assess hepatic fat and iron content, respectively. Multiparametric MRI was able to highlight a more effective reduction of both imaging biomarkers compared to mice treated with a monoagonist, in correlation with histologic findings [147]. In particular, these findings shed new light on the potential value of regulating iron homeostasis as a therapeutic strategy for MASLD.

Current trends suggest that non-invasive detection of early stages of MASLD can improve treatment success. In line with this evidence, assessment of hepatic β-oxidation by [D15]-octanoate metabolism analysis and deuterium detection by MRI are emerging as translatable imaging modalities to study the clinical course of MASLD. Interestingly, HF-fed C57BL/6J mice were monitored by 11 T MRI after tail vein injection of [D15]-octanoate for up to 36 weeks. Decreased β-oxidative efficiency in fatty liver has been shown to be useful for monitoring the progression of MASLD, as it occurs before overt structural changes such as hepatomegaly [148].

Advanced MRI techniques have also been successfully applied to GEMs to better understand the role of specific genes in the onset and progression of MASLD or to develop precision medicine therapeutic strategies.

Dixon- and STEAM-based, proton density MRS protocols were applied on 3T scanners in an HFD-fed *eNOS* KO mouse model, to noninvasively characterize hepatic fatty acid changes and assess the response to metformin treatment.

KO mice showed increased hepatic fat accumulation compared to control mice after 8 weeks of HFD, while metformin treatment significantly improved the hepatic lipidomic profile compared to untreated mice [149]. In WD-fed female B6.Cg-Lepob/J mice, the combination of 1H-based liver fat fraction and 19F-based inflammation measurements using an 11.7 T small animal imaging scanner and Kupffer cells uptake of perfluorocarbon demonstrated the complementary utility of longitudinal quantification of multiple MRI biomarkers of disease to study MASLD liver pathology [150].

In summary, imaging may provide robust, non-invasive, and quantitative results that are essential for the comprehensive and ethical study of hepatic steatosis progression and treatment in mouse models; unfortunately, it does not provide information on its microscopic characteristics, such as hepatocyte ballooning, lobular inflammation, Mallory bodies, and microvesicular and macrovesicular steatosis. Therefore, they cannot yet fully replace histological analysis of the liver obtained through sampling or biopsy. In particular, the assessment of histological features is a crucial step in mouse models to understand how well the model reflects human disease. In this perspective, the complementary use of imaging and histological analyses may represent a key strategy to obtain multiparametric information in an accurate and longitudinal manner, using the smallest possible number of mice.

5. Conclusions

Given the multifactorial and heterogeneous nature of MASLD in humans, no single animal model can adequately capture the full spectrum of disease manifestations. Instead, the rational selection of fit-for-purpose mouse models—guided by clinically relevant metabolic, histological, and non-invasive endpoints—is essential to address specific mechanistic and therapeutic questions. Such a multimodal strategy will address the limitations of single approaches by capturing complementary biological insights.

Liver biopsy remains irreplaceable for the definitive diagnosis of steatohepatitis and can help exclude alternative causes of liver disease, but its invasiveness and sampling variability limit its suitability for monitoring disease progression over time. On the other hand, imaging is becoming essential for precision medicine approaches in MASLD, allowing for comprehensive, non-invasive assessment and integration with clinical data for risk stratification, improving individualized care and treatment monitoring. Given the chronic and progressive nature of MASLD, longitudinal assessment with non-invasive tools such as imaging techniques is strongly recommended in patients to monitor disease progression, assess response to therapies, and predict the risk of liver-related events and overall health.

Although no single mouse model perfectly reproduces every aspect of human MASLD, mice remain indispensable for research due to their ability to reproduce complex interactions between multiple organs that simpler systems cannot replicate. Recent advances in mouse models include the induction of disease through diets that closely mimic human Western dietary patterns, leading to metabolic syndrome; clinically relevant genetic modifications; evaluation of host-microbiota interactions; and environmental standardization, often combined in integrated approaches. In this context, knowledge of comparative pathology and the use of translational diagnostic tools are essential to improve research outcomes. Therefore, this review aimed to summarize current evidence from the literature on mouse models of MASLD, focusing on comparative histology, and highlight recent advances in translational imaging, contributing to bridging the gap between human disease and preclinical research. The standardization of experimental methods in model generation and the harmonization of imaging protocols are expected to improve reproducibility, support the 3R principles, and enhance the predictive value of preclinical studies, ultimately accelerating the development of effective therapeutic strategies for MASLD.

Looking forward, future research in both humans and mice is expected to increasingly rely on stratified, phenotype-driven approaches that integrate histology, quantitative imaging, and metabolic profiling. In clinical settings, this will enable more precise patient classification and the use of non-invasive tools to monitor disease progression and therapeutic response. In parallel, preclinical research is likely to expand the use of longitudinal imaging-based study designs, combined disease models (genetic, diet, and environmental factors), and humanized mouse models, including those incorporating human hepatocytes, immune components, or microbiota, to more faithfully recapitulate human-specific metabolic and inflammatory features of MASLD. Together, these advances will promote a more aligned, predictive, and personalized translational framework, ultimately improving the success of MASLD drug development and facilitating the implementation of multifactorial and combination-based therapeutic strategies.

6. Limitations

This review has some limitations that should be addressed. Although efforts were made to provide a comprehensive overview of recent advances in murine models and preclinical imaging applications for MASLD, the possibility of literature selection bias cannot be completely excluded due to database selection and inclusion criteria. Moreover, the field is rapidly evolving, and newly published studies may further expand or refine the

concepts discussed. Finally, variability among experimental models and methodologies may limit the direct comparability of findings across studies.

Author Contributions: Conceptualization, D.B., S.G., L.L., M.G. and V.B.; writing—original draft preparation, D.B., S.G., L.L., T.T., M.G. and V.B.; writing—review and editing, D.B., S.G., L.L., T.T., M.G., L.G., L.F., G.I., M.C. and V.B.; supervision, D.B., S.G., L.L., M.G., M.C. and V.B. All authors have read and agreed to the published version of the manuscript.

Funding: This research received no external funding.

Institutional Review Board Statement: Not applicable.

Informed Consent Statement: Not applicable.

Data Availability Statement: No new data were created or analyzed in this study.

Conflicts of Interest: The authors declare no conflicts of interest.

Abbreviations

The following abbreviations are used in this manuscript:

ALD	Alcoholic Liver Disease
IR	Insulin Resistance
MASLD	Metabolic Dysfunction-Associated Steatotic Liver Disease
NAFLD	Non-Alcoholic Fatty Liver Disease
MASH	Metabolic Dysfunction-Associated Steatohepatitis
HCC	Hepatocellular carcinoma
BMI	Body mass index
PNPLA3	Patatin-like phospholipase domain-containing 3
HSD17B13	17β-hydroxysteroid dehydrogenase-13
GCRK	Glucokinase regulatory protein gene
MBOAT7	Membrane-bound O-acyltransferase domain–containing 7
GLP-1R	Glucagon-like peptide-receptor 1
PPAR	Peroxisome proliferator-activated receptor
HFD	High fat diet
MCD	Methionine and choline deficient diet
CD	Choline deficient diet
CAFD	Cafeteria diet
WD	Western diet
GEM	Genetically engineered mouse
KO	Knock-out
GAN	Gubra Amylin diet for non-alcoholic steatohepatitis
TN	Thermoneutrality
NZO	New Zealand Obese
SD	Standard Diet
MAPK15	Mitogen-activated protein kinase 15
Atg7	Autophagy-related gene 7
AKAP1	A-kinase anchoring protein 1
ACSL1	Acyl-CoA synthetase long-chain family member 1
GPAT1	Glycerol-3-phosphate acyltransferase 1
Ay	Agouti Yellow
DKO	Cyp2a12/Cyp2c70 knock-out
BW	Body weight
ER	Endoplasmic reticulum
HSC	Hepatic stellate cells

H&E	Hematoxylin & Eosin
NAS	NAFLD Activity Score
SAF	Steatosis, Activity and Fibrosis
NIT	Non-invasive test
US	Ultrasound
CT	Computed tomography
MRI	Magnetic resonance imaging
HVPG	Hepatic venous pressure gradient
EUS-LB	Endoscopic ultrasound-guided liver biopsy
FNA	Fine-needle aspiration
FNB	Fine-needle biopsy
AI	Artificial intelligence
WFUMB	World Federation for Ultrasound in Medicine and Biology
MRI-PDFF	Magnetic resonance imaging proton density fat fraction
MRS	Magnetic resonance spectroscopy
QUS	Quantitative ultrasound
HRI	Hepatorenal index
ATI	Attenuation imaging
BSC	Backscattered coefficient
SoS	Speed of sound
SWE	Share wave elastography
RTE	Real time elastography
dMRI	Diffusion-based magnetic resonance imaging
DCE	Dynamic contrast enhanced
STEAM	Stimulated echo acquisition mode
VAPOR	Variable power radiofrequency pulses with optimized relaxation delays
GC-MS	Gas chromatography-mass spectrometry
PEG-FGF21v	Polyethylene glycol fibroblast growth factor 21 variant

References

1. Aron-Wisnewsky, J.; Vigliotti, C.; Witjes, J.; Le, P.; Holleboom, A.G.; Verheij, J.; Nieuwdorp, M.; Clément, K. Gut Microbiota and Human NAFLD: Disentangling Microbial Signatures from Metabolic Disorders. *Nat. Rev. Gastroenterol. Hepatol.* **2020**, *17*, 279–297. [CrossRef]
2. Rinella, M.E.; Lazarus, J.V.; Ratziu, V.; Francque, S.M.; Sanyal, A.J.; Kanwal, F.; Romero, D.; Abdelmalek, M.F.; Anstee, Q.M.; Arab, J.P.; et al. A Multisociety Delphi Consensus Statement on New Fatty Liver Disease Nomenclature. *Hepatology* **2023**, *78*, 1966–1986. [CrossRef]
3. Stevanović-Silva, J.; Beleza, J.; Coxito, P.; Costa, R.C.; Ascensão, A.; Magalhães, J. Fit Mothers for a Healthy Future: Breaking the Intergenerational Cycle of Non-alcoholic Fatty Liver Disease with Maternal Exercise. *Eur. J. Clin. Investig.* **2022**, *52*, e13596. [CrossRef] [PubMed]
4. Maliken, B.D.; Nelson, J.E.; Klintworth, H.M.; Beauchamp, M.; Yeh, M.M.; Kowdley, K.V. Hepatic Reticuloendothelial System Cell Iron Deposition Is Associated with Increased Apoptosis in Nonalcoholic Fatty Liver Disease. *Hepatology* **2013**, *57*, 1806–1813. [CrossRef] [PubMed]
5. Younossi, Z.M.; Golabi, P.; Paik, J.M.; Henry, A.; Van Dongen, C.; Henry, L. The Global Epidemiology of Nonalcoholic Fatty Liver Disease (NAFLD) and Nonalcoholic Steatohepatitis (NASH): A Systematic Review. *Hepatology* **2023**, *77*, 1335–1347. [CrossRef]
6. Huo, Z.; Chen, Y.; Huang, Y.; Yang, Z.; Long, Y.; Zhang, Q.; Chen, S.; Wang, G.; Zhu, S.; Sun, D.; et al. Long-Term Prognosis of Lean MASLD: Evidence from Three Population-Based Prospective Cohorts. *Gut* **2025**, *75*, 772–785. [CrossRef]
7. Ha, S.; Wong, V.W.-S.; Zhang, X.; Yu, J. Interplay between Gut Microbiome, Host Genetic and Epigenetic Modifications in MASLD and MASLD-Related Hepatocellular Carcinoma. *Gut* **2024**, *74*, 141–152. [CrossRef]
8. Jegodzinski, L.; Rudolph, L.; Castven, D.; Sayk, F.; Rout, A.K.; Föh, B.; Hölzen, L.; Meyhöfer, S.; Schenk, A.; Weber, S.N.; et al. *PNPLA3* I148M Variant Links to Adverse Metabolic Traits in MASLD during Fasting and Feeding. *JHEP Rep.* **2025**, *7*, 101450. [CrossRef]
9. Su, W.; Wang, Y.; Jia, X.; Wu, W.; Li, L.; Tian, X.; Li, S.; Wang, C.; Xu, H.; Cao, J.; et al. Comparative Proteomic Study Reveals 17β-HSD13 as a Pathogenic Protein in Nonalcoholic Fatty Liver Disease. *Proc. Natl. Acad. Sci. USA* **2014**, *111*, 11437–11442. [CrossRef] [PubMed]

10. Orho-Melander, M.; Melander, O.; Guiducci, C.; Perez-Martinez, P.; Corella, D.; Roos, C.; Tewhey, R.; Rieder, M.J.; Hall, J.; Abecasis, G.; et al. Common Missense Variant in the Glucokinase Regulatory Protein Gene Is Associated with Increased Plasma Triglyceride and C-Reactive Protein but Lower Fasting Glucose Concentrations. *Diabetes* **2008**, *57*, 3112–3121. [CrossRef]
11. Chandrasekaran, P.; Weiskirchen, R. The Pivotal Role of the Membrane-Bound O-Acyltransferase Domain Containing 7 in Non-Alcoholic Fatty Liver Disease. *Livers* **2023**, *4*, 1–14. [CrossRef]
12. O'Hare, E.A.; Yang, R.; Yerges-Armstrong, L.M.; Sreenivasan, U.; McFarland, R.; Leitch, C.C.; Wilson, M.H.; Narina, S.; Gorden, A.; Ryan, K.A.; et al. *TM6SF2* Rs58542926 Impacts Lipid Processing in Liver and Small Intestine. *Hepatology* **2017**, *65*, 1526–1542. [CrossRef] [PubMed]
13. Nemer, M.; Osman, F.; Said, A. Dietary Macro and Micronutrients Associated with MASLD: Analysis of a National US Cohort Database. *Ann. Hepatol.* **2024**, *29*, 101491. [CrossRef] [PubMed]
14. Kovynev, A.; Charchuta, M.M.; Begtašević, A.; Ducarmon, Q.R.; Rensen, P.C.N.; Schönke, M. Combination of Dietary Fiber and Exercise Training Improves Fat Loss in Mice but Does Not Ameliorate MASLD More than Exercise Alone. *Am. J. Physiol.-Gastrointest. Liver Physiol.* **2025**, *328*, G399–G410. [CrossRef]
15. Jung, S.; Bae, H.; Song, W.-S.; Chun, Y.; Le, J.; Alam, Y.; Verlande, A.; Chun, S.K.; Kim, J.; Kelly, M.E.; et al. Dietary Fibre-Adapted Gut Microbiome Clears Dietary Fructose and Reverses Hepatic Steatosis. *Nat. Metab.* **2025**, *7*, 1801–1818. [CrossRef]
16. Shen, F.; Zheng, R.-D.; Sun, X.-Q.; Ding, W.-J.; Wang, X.-Y.; Fan, J.-G. Gut Microbiota Dysbiosis in Patients with Non-Alcoholic Fatty Liver Disease. *Hepatobiliary Pancreat. Dis. Int.* **2017**, *16*, 375–381. [CrossRef]
17. Hong, F.; Radaeva, S.; Pan, H.; Tian, Z.; Veech, R.; Gao, B. Interleukin 6 Alleviates Hepatic Steatosis and Ischemia/Reperfusion Injury in Mice with Fatty Liver Disease. *Hepatology* **2004**, *40*, 933–941. [CrossRef]
18. Zheng, Y.; Huang, C.; Zhao, L.; Chen, Y.; Liu, F. Regulation of Decorin by Ursolic Acid Protects against Non-Alcoholic Steatohepatitis. *Biomed. Pharmacother.* **2021**, *143*, 112166. [CrossRef]
19. Drygalski, K. Pharmacological Treatment of MASLD: Contemporary Treatment and Future Perspectives. *Int. J. Mol. Sci.* **2025**, *26*, 6518. [CrossRef]
20. Hudson, D.; Afzaal, T.; Bualbanat, H.; AlRamdan, R.; Howarth, N.; Parthasarathy, P.; AlDarwish, A.; Stephenson, E.; Almahanna, Y.; Hussain, M.; et al. Modernizing Metabolic Dysfunction-Associated Steatotic Liver Disease Diagnostics: The Progressive Shift from Liver Biopsy to Noninvasive Techniques. *Ther. Adv. Gastroenterol.* **2024**, *17*, 17562848241276334. [CrossRef]
21. Tacke, F.; Horn, P.; Wai-Sun Wong, V.; Ratziu, V.; Bugianesi, E.; Francque, S.; Zelber-Sagi, S.; Valenti, L.; Roden, M.; Schick, F.; et al. EASL–EASD–EASO Clinical Practice Guidelines on the Management of Metabolic Dysfunction-Associated Steatotic Liver Disease (MASLD). *J. Hepatol.* **2024**, *81*, 492–542. [CrossRef]
22. Gargiulo, S.; Gramanzini, M.; Bonente, D.; Tamborrino, T.; Inzalaco, G.; Gherardini, L.; Franci, L.; Bertelli, E.; Barone, V.; Chiariello, M. Preclinical Application of Computer-Aided High-Frequency Ultrasound (HFUS) Imaging: A Preliminary Report on the In Vivo Characterization of Hepatic Steatosis Progression in Mouse Models. *J. Imaging* **2025**, *11*, 369. [CrossRef] [PubMed]
23. Pelechá, M.; Villanueva-Bádenas, E.; Timor-López, E.; Donato, M.T.; Tolosa, L. Cell Models and Omics Techniques for the Study of Nonalcoholic Fatty Liver Disease: Focusing on Stem Cell-Derived Cell Models. *Antioxidants* **2021**, *11*, 86. [CrossRef]
24. Caddeo, A.; Maurotti, S.; Kovooru, L.; Romeo, S. 3D Culture Models to Study Pathophysiology of Steatotic Liver Disease. *Atherosclerosis* **2024**, *393*, 117544. [CrossRef] [PubMed]
25. Youhanna, S.; Taebnia, N.; Liang, Y.; Cheng, N.; Wang, Y.; Michel, M.; Lauschke, V.M. Primary Human Tissue Models for Metabolic Dysfunction-Associated Liver Disease—Toward Streamlining Drug Discovery with Patient-Derived Assays. *Adv. Biol.* **2025**, *9*, e00337. [CrossRef]
26. Kwon, Y.; Gottmann, P.; Wang, S.; Tissink, J.; Motzler, K.; Sekar, R.; Albrecht, W.; Cadenas, C.; Hengstler, J.G.; Schürmann, A.; et al. Induction of Steatosis in Primary Human Hepatocytes Recapitulates Key Pathophysiological Aspects of Metabolic Dysfunction-Associated Steatotic Liver Disease. *J. Hepatol.* **2025**, *82*, 18–27. [CrossRef] [PubMed]
27. Kruepunga, N.; Hakvoort, T.B.M.; Hikspoors, J.P.J.M.; Köhler, S.E.; Lamers, W.H. Anatomy of Rodent and Human Livers: What Are the Differences? *Biochim. Biophys. Acta (BBA)-Mol. Basis Dis.* **2019**, *1865*, 869–878. [CrossRef]
28. Luo, Y.; Lu, H.; Peng, D.; Ruan, X.; Eugene Chen, Y.; Guo, Y. Liver-humanized Mice: A Translational Strategy to Study Metabolic Disorders. *J. Cell. Physiol.* **2022**, *237*, 489–506. [CrossRef]
29. Nagarajan, P. Genetically Modified Mouse Models for the Study of Nonalcoholic Fatty Liver Disease. *World J. Gastroenterol.* **2012**, *18*, 1141. [CrossRef]
30. Jahn, D.; Kircher, S.; Hermanns, H.M.; Geier, A. Animal Models of NAFLD from a Hepatologist's Point of View. *Biochim. Biophys. Acta (BBA)-Mol. Basis Dis.* **2019**, *1865*, 943–953. [CrossRef]
31. Flessa, C.-M.; Nasiri-Ansari, N.; Kyrou, I.; Leca, B.M.; Lianou, M.; Chatzigeorgiou, A.; Kaltsas, G.; Kassi, E.; Randeva, H.S. Genetic and Diet-Induced Animal Models for Non-Alcoholic Fatty Liver Disease (NAFLD) Research. *Int. J. Mol. Sci.* **2022**, *23*, 15791. [CrossRef]
32. Fu, Y.; Hua, Y.; Alam, N.; Liu, E. Progress in the Study of Animal Models of Metabolic Dysfunction-Associated Steatotic Liver Disease. *Nutrients* **2024**, *16*, 3120. [CrossRef]

33. Cui, X.; Li, H.; Li, L.; Xie, C.; Gao, J.; Chen, Y.; Zhang, H.; Hao, W.; Fu, J.; Guo, H. Rodent Model of Metabolic Dysfunction-associated Fatty Liver Disease: A Systematic Review. *J. Gastroenterol. Hepatol.* **2025**, *40*, 48–66. [CrossRef]
34. Vacca, M.; Kamzolas, I.; Harder, L.M.; Oakley, F.; Trautwein, C.; Hatting, M.; Ross, T.; Bernardo, B.; Oldenburger, A.; Hjuler, S.T.; et al. An Unbiased Ranking of Murine Dietary Models Based on Their Proximity to Human Metabolic Dysfunction-Associated Steatotic Liver Disease (MASLD). *Nat. Metab.* **2024**, *6*, 1178–1196. [CrossRef] [PubMed]
35. Chen, J.; Jiang, X. A High-Fructose Diet Leads to Osteoporosis by Suppressing the Expression of *Thrb* and Facilitating the Accumulation of Cholesterol. *Cell Death Discov.* **2025**, *11*, 159. [CrossRef]
36. Estévez-Vázquez, O.; Benedé-Ubieto, R.; Guo, F.; Gómez-Santos, B.; Aspichueta, P.; Reissing, J.; Bruns, T.; Sanz-García, C.; Sydor, S.; Bechmann, L.P.; et al. Fat: Quality, or Quantity? What Matters Most for the Progression of Metabolic Associated Fatty Liver Disease (MAFLD). *Biomedicines* **2021**, *9*, 1289. [CrossRef]
37. Nielsen, M.H.; Nøhr-Meldgaard, J.; Møllerhøj, M.B.; Oró, D.; Pors, S.E.; Andersen, M.W.; Kamzolas, I.; Petsalaki, E.; Vacca, M.; Harder, L.M.; et al. Characterization of Six Clinical Drugs and Dietary Intervention in the Nonobese CDAA-HFD Mouse Model of MASH and Progressive Fibrosis. *Am. J. Physiol.-Gastrointest. Liver Physiol.* **2025**, *328*, G51–G71. [CrossRef]
38. Li, H.; Toth, E.; Cherrington, N.J. Asking the Right Questions with Animal Models: Methionine- and Choline-Deficient Model in Predicting Adverse Drug Reactions in Human NASH. *Toxicol. Sci.* **2018**, *161*, 23–33. [CrossRef]
39. Fang, T.; Wang, H.; Pan, X.; Little, P.J.; Xu, S.; Weng, J. Mouse Models of Nonalcoholic Fatty Liver Disease (NAFLD): Pathomechanisms and Pharmacotherapies. *Int. J. Biol. Sci.* **2022**, *18*, 5681–5697. [CrossRef] [PubMed]
40. Drescher, H.K.; Weiskirchen, R.; Fülöp, A.; Hopf, C.; De San Román, E.G.; Huesgen, P.F.; De Bruin, A.; Bongiovanni, L.; Christ, A.; Tolba, R.; et al. The Influence of Different Fat Sources on Steatohepatitis and Fibrosis Development in the Western Diet Mouse Model of Non-Alcoholic Steatohepatitis (NASH). *Front. Physiol.* **2019**, *10*, 770. [CrossRef] [PubMed]
41. Saraswathi, V.; Kumar, N.; Ai, W.; Gopal, T.; Bhatt, S.; Harris, E.N.; Talmon, G.A.; Desouza, C.V. Myristic Acid Supplementation Aggravates High Fat Diet-Induced Adipose Inflammation and Systemic Insulin Resistance in Mice. *Biomolecules* **2022**, *12*, 739. [CrossRef] [PubMed]
42. Pompili, S.; Vetuschi, A.; Gaudio, E.; Tessitore, A.; Capelli, R.; Alesse, E.; Latella, G.; Sferra, R.; Onori, P. Long-Term Abuse of a High-Carbohydrate Diet Is as Harmful as a High-Fat Diet for Development and Progression of Liver Injury in a Mouse Model of NAFLD/NASH. *Nutrition* **2020**, *75*, 110782. [CrossRef] [PubMed]
43. Maddie, N.; Chacko, N.; Matatov, D.; Carrillo-Sepulveda, M.A. Western Diet Promotes the Progression of Metabolic Dysfunction-associated Steatotic Liver Disease in Association with Ferroptosis in Male Mice. *Physiol. Rep.* **2024**, *12*, e70139. [CrossRef]
44. Meijnikman, A.S.; Fondevila, M.F.; Arrese, M.; Kisseleva, T.; Bataller, R.; Schnabl, B. Towards More Consistent Models and Consensual Terminology in Preclinical Research for Steatotic Liver Disease. *J. Hepatol.* **2025**, *82*, 760–766. [CrossRef] [PubMed]
45. Svobodová, G.; Horní, M.; Velecká, E.; Boušová, I. Metabolic Dysfunction-Associated Steatotic Liver Disease-Induced Changes in the Antioxidant System: A Review. *Arch. Toxicol.* **2025**, *99*, 1–22. [CrossRef]
46. Ma, X.; Bian, W.; Song, W.; Lu, Y.; Wang, Z.; Yao, Z.; Xuan, Q. Metabolome Profiling across Liver Lobes and Metabolic Shifts of the MASLD Mice. *Genes. Nutr.* **2025**, *20*, 9. [CrossRef] [PubMed]
47. Li, Y.-Q.; Huang, C.; Chen, J.; Yang, S.; Cheng, J.; Chen, H.; Zhou, Y. Identification of the Role of Sugar-Sweetened Beverages in the Progression of a Murine Metabolic Dysfunction-Associated Steatotic Liver Disease Model. *Front. Nutr.* **2025**, *12*, 1710267. [CrossRef]
48. Jeon, H.J.; Rou, W.S.; Kim, S.H.; Lee, B.S.; Kim, H.N.; Choi, H.-G.; Seo, J.; Eun, H.S.; Jung, S. Sugar-Sweetened Beverage Consumption and Metabolic Dysfunction-Associated Steatotic Liver Disease: A Beverage Type-Specific Analysis Using Korea National Health and Nutrition Examination Survey. *Epidemiol. Health* **2025**, *47*, e2025038. [CrossRef]
49. Hsu, W.-F.; Lee, M.-H.; Lii, C.-K.; Peng, C.-Y. No Difference in Liver Damage Induced by Isocaloric Fructose or Glucose in Mice with a High-Fat Diet. *Nutrients* **2024**, *16*, 3571. [CrossRef]
50. Zhang, Z.; Qin, X.; Yi, T.; Li, Y.; Li, C.; Zeng, M.; Luo, H.; Lin, X.; Xie, J.; Xia, B.; et al. Gubra Amylin-NASH Diet Induced Nonalcoholic Fatty Liver Disease Associated with Histological Damage, Oxidative Stress, Immune Disorders, Gut Microbiota, and Its Metabolic Dysbiosis in Colon. *Mol. Nutr. Food Res.* **2024**, *68*, 2300845. [CrossRef]
51. Green, C.D.; Weigel, C.; Brown, R.D.R.; Bedossa, P.; Dozmorov, M.; Sanyal, A.J.; Spiegel, S. A New Preclinical Model of Western Diet-induced Progression of Non-alcoholic Steatohepatitis to Hepatocellular Carcinoma. *FASEB J.* **2022**, *36*, e22372. [CrossRef]
52. Makri, E.S.; Xanthopoulos, K.; Mavrommatis Parasidis, P.; Makri, E.; Pettas, S.; Tsingotjidou, A.; Cheva, A.; Ballaouri, I.; Gerou, S.; Goulas, A.; et al. Partial Validation of a Six-Month High-Fat Diet and Fructose-Glucose Drink Combination as a Mouse Model of Nonalcoholic Fatty Liver Disease. *Endocrine* **2024**, *85*, 704–716. [CrossRef]
53. Khoj, D.; Huang, R.; Altvater, E.; Ishfaq, Z.N.; Jiang, X.; Axen, K.V.; Caviglia, J.M. Mouse Model of Metabolic Dysfunction-Associated Steatotic Liver Disease with Fibrosis. *J. Vis. Exp.* **2025**, *221*, 68294. [CrossRef] [PubMed]
54. Hansen, H.H.; Ægidius, H.M.; Oró, D.; Evers, S.S.; Heebøll, S.; Eriksen, P.L.; Thomsen, K.L.; Bengtsson, A.; Veidal, S.S.; Feigh, M.; et al. Human Translatability of the GAN Diet-Induced Obese Mouse Model of Non-Alcoholic Steatohepatitis. *BMC Gastroenterol.* **2020**, *20*, 210. [CrossRef]

55. Dutta, S.; Sengupta, P. Men and Mice: Relating Their Ages. *Life Sci.* **2016**, *152*, 244–248. [CrossRef]
56. Jackson, S.J.; Andrews, N.; Ball, D.; Bellantuono, I.; Gray, J.; Hachoumi, L.; Holmes, A.; Latcham, J.; Petrie, A.; Potter, P.; et al. Does Age Matter? The Impact of Rodent Age on Study Outcomes. *Lab. Anim.* **2017**, *51*, 160–169. [CrossRef] [PubMed]
57. Li, X.; Lu, Y.; Liang, X.; Zhou, X.; Li, D.; Zhang, Z.; Niu, Y.; Liu, S.; Ye, L.; Zhang, R. A New NASH Model in Aged Mice with Rapid Progression of Steatohepatitis and Fibrosis. *PLoS ONE* **2023**, *18*, e0286257. [CrossRef]
58. Hansen, H.H.; Pors, S.; Andersen, M.W.; Vyberg, M.; Nøhr-Meldgaard, J.; Nielsen, M.H.; Oró, D.; Madsen, M.R.; Lewinska, M.; Møllerhøj, M.B.; et al. Semaglutide Reduces Tumor Burden in the GAN Diet-Induced Obese and Biopsy-Confirmed Mouse Model of NASH-HCC with Advanced Fibrosis. *Sci. Rep.* **2023**, *13*, 23056. [CrossRef]
59. Reeves, P.G. Components of the AIN-93 Diets as Improvements in the AIN-76A Diet. *J. Nutr.* **1997**, *127*, 838S–841S. [CrossRef]
60. Aguiar, L.M.; Moura, C.S.D.; Ballard, C.R.; Roquetto, A.R.; Silva Maia, J.K.D.; Duarte, G.H.B.; Costa, L.B.E.D.; Torsoni, A.S.; Amaya-Farfan, J.; Maróstica Junior, M.R.; et al. Metabolic Dysfunctions Promoted by AIN-93G Standard Diet Compared with Three Obesity-Inducing Diets in C57BL/6J Mice. *Curr. Res. Physiol.* **2022**, *5*, 436–444. [CrossRef] [PubMed]
61. Almeida-Suhett, C.P.; Scott, J.M.; Graham, A.; Chen, Y.; Deuster, P.A. Control Diet in a High-Fat Diet Study in Mice: Regular Chow and Purified Low-Fat Diet Have Similar Effects on Phenotypic, Metabolic, and Behavioral Outcomes. *Nutr. Neurosci.* **2019**, *22*, 19–28. [CrossRef]
62. Benegiamo, G.; Von Alvensleben, G.V.G.; Rodríguez-López, S.; Goeminne, L.J.E.; Bachmann, A.M.; Morel, J.-D.; Broeckx, E.; Ma, J.Y.; Carreira, V.; Youssef, S.A.; et al. The Genetic Background Shapes the Susceptibility to Mitochondrial Dysfunction and NASH Progression. *J. Exp. Med.* **2023**, *220*, e20221738. [CrossRef] [PubMed]
63. Hupa-Breier, K.L.; Schenk, H.; Campos-Murguia, A.; Wellhöner, F.; Heidrich, B.; Dywicki, J.; Hartleben, B.; Böker, C.; Mall, J.; Terkamp, C.; et al. Novel Translational Mouse Models of Metabolic Dysfunction-Associated Steatotic Liver Disease Comparable to Human MASLD with Severe Obesity. *Mol. Metab.* **2025**, *93*, 102104. [CrossRef]
64. Lee, Y.-C.; Lee, H.S.; Jeon, S.; Lee, Y.-J.; Kwon, Y.-J.; Lee, J.-W. Assessing Nutritional Factors for Metabolic Dysfunction-Associated Steatotic Liver Disease via Diverse Statistical Tools. *Diabetes Metab. J.* **2026**, *50*, 178–189. [CrossRef] [PubMed]
65. Mann, J.P.; Semple, R.K.; Armstrong, M.J. How Useful Are Monogenic Rodent Models for the Study of Human Non-Alcoholic Fatty Liver Disease? *Front. Endocrinol.* **2016**, *7*, 145. [CrossRef]
66. Hintze, K.J.; Benninghoff, A.D.; Cho, C.E.; Ward, R.E. Modeling the Western Diet for Preclinical Investigations. *Adv. Nutr.* **2018**, *9*, 263–271. [CrossRef]
67. Martin, C.M.P.; Polizzi, A.; Alquier-Bacquié, V.; Huillet, M.; Rives, C.; Dauriat, C.J.G.; Bruse, J.; Melin, V.; Naylies, C.; Lippi, Y.; et al. Thermoneutral Housing Worsens MASLD and Reveals Defective Brown Adipose Tissue Response to B3-Adrenergic Stimulation. *iScience* **2025**, *28*, 113221. [CrossRef]
68. Blok, N.B.; Myronovych, A.; McMahon, G.; Bozadjieva-Kramer, N.; Seeley, R.J. The Evolution of Steatosis and Fibrosis in Mice on a MASH-Inducing Diet and the Effects of Housing Temperature. *Am. J. Physiol.-Endocrinol. Metab.* **2025**, *328*, E513–E523. [CrossRef]
69. Jancova, P.; Ismail, K.; Vistejnova, L. Relationship between MASLD and Women's Health: A Review. *Womens Health* **2025**, *21*, 17455057251376883. [CrossRef]
70. Alves, E.S.; Santos, J.D.M.; Cruz, A.G.; Camargo, F.N.; Talarico, C.H.Z.; Santos, A.R.M.; Silva, C.A.A.; Morgan, H.J.N.; Matos, S.L.; Araujo, L.C.C.; et al. Hepatic Estrogen Receptor Alpha Overexpression Protects Against Hepatic Insulin Resistance and MASLD. *Pathophysiology* **2025**, *32*, 1. [CrossRef] [PubMed]
71. Manjarrés, L.; Xavier, A.; González, L.; Garrido, C.; Zacconi, F.C.; Rivera, K.; Parra, L.; Phinikaridou, A.; Besa, C.; Andia, M.E. Sex Differences in the Relationship between Body Composition and MASLD Progression in a Murine Model of Metabolic Syndrome. *iScience* **2025**, *28*, 111863. [CrossRef]
72. Korovila, I.; Höhn, A.; Jung, T.; Grune, T.; Ott, C. Reduced Liver Autophagy in High-Fat Diet Induced Liver Steatosis in New Zealand Obese Mice. *Antioxidants* **2021**, *10*, 501. [CrossRef]
73. Inzalaco, G.; Gargiulo, S.; Bonente, D.; Gherardini, L.; Franci, L.; Lorito, N.; Del Turco, S.; Tatoni, D.; Tamborrino, T.; Galvagni, F.; et al. *MAPK15* Controls Intracellular Lipid Uptake and Protects Mammalian Liver from Steatotic Disease. *Hepatol. Commun.* **2026**, *10*, e0870. [CrossRef]
74. Sakane, S.; Hikita, H.; Shirai, K.; Myojin, Y.; Sasaki, Y.; Kudo, S.; Fukumoto, K.; Mizutani, N.; Tahata, Y.; Makino, Y.; et al. White Adipose Tissue Autophagy and Adipose-Liver Crosstalk Exacerbate Nonalcoholic Fatty Liver Disease in Mice. *Cell. Mol. Gastroenterol. Hepatol.* **2021**, *12*, 1683–1699. [CrossRef] [PubMed]
75. Ji, L.; Zhao, Y.; He, L.; Zhao, J.; Gao, T.; Liu, F.; Qi, B.; Kang, F.; Wang, G.; Zhao, Y.; et al. *X1AKAP1* Deficiency Attenuates Diet-Induced Obesity and Insulin Resistance by Promoting Fatty Acid Oxidation and Thermogenesis in Brown Adipocytes. *Adv. Sci.* **2022**, *9*, 2204669. [CrossRef] [PubMed]
76. He, L.; She, X.; Guo, L.; Gao, M.; Wang, S.; Lu, Z.; Guo, H.; Li, R.; Nie, Y.; Xing, J.; et al. Hepatic AKAP1 Deficiency Exacerbates Diet-Induced MASLD by Enhancing GPAT1-Mediated Lysophosphatidic Acid Synthesis. *Nat. Commun.* **2025**, *16*, 4286. [CrossRef] [PubMed]

77. Gargiulo, S.; Barone, V.; Bonente, D.; Tamborrino, T.; Inzalaco, G.; Gherardini, L.; Bertelli, E.; Chiariello, M. Integrated Ultrasound Characterization of the Diet-Induced Obesity (DIO) Model in Young Adult C57bl/6j Mice: Assessment of Cardiovascular, Renal and Hepatic Changes. *J. Imaging* **2024**, *10*, 217. [CrossRef]
78. Burelle, C.; Clapatiuc, V.; Deschênes, S.; Cuillerier, A.; De Loof, M.; Higgins, M.-È.; Boël, H.; Daneault, C.; Chouinard, B.; Clavet, M.-É.; et al. A Genetic Mouse Model of Lean-NAFLD Unveils Sexual Dimorphism in the Liver-Heart Axis. *Commun. Biol.* **2024**, *7*, 356. [CrossRef]
79. Zhang, X.; Lau, H.C.-H.; Ha, S.; Liu, C.; Liang, C.; Lee, H.W.; Ng, Q.W.-Y.; Zhao, Y.; Ji, F.; Zhou, Y.; et al. Intestinal *TM6SF2* Protects against Metabolic Dysfunction-Associated Steatohepatitis through the Gut–Liver Axis. *Nat. Metab.* **2025**, *7*, 102–119. [CrossRef]
80. Fisher-Wellman, K.H.; Ryan, T.E.; Smith, C.D.; Gilliam, L.A.A.; Lin, C.-T.; Reese, L.R.; Torres, M.J.; Neufer, P.D. A Direct Comparison of Metabolic Responses to High-Fat Diet in C57BL/6J and C57BL/6NJ Mice. *Diabetes* **2016**, *65*, 3249–3261. [CrossRef]
81. Ueda, H.; Honda, A.; Miyazaki, T.; Morishita, Y.; Hirayama, T.; Iwamoto, J.; Ikegami, T. High-Fat/High-Sucrose Diet Results in a High Rate of MASH with HCC in a Mouse Model of Human-like Bile Acid Composition. *Hepatol. Commun.* **2025**, *9*, e0606. [CrossRef] [PubMed]
82. Takahashi, Y. Histopathology of Nonalcoholic Fatty Liver Disease/Nonalcoholic Steatohepatitis. *World J. Gastroenterol.* **2014**, *20*, 15539. [CrossRef]
83. Brown, G.T.; Kleiner, D.E. Histopathology of Nonalcoholic Fatty Liver Disease and Nonalcoholic Steatohepatitis. *Metabolism* **2016**, *65*, 1080–1086. [CrossRef]
84. Goodman, Z.D. Role of Liver Biopsy in Clinical Trials and Clinical Management of Nonalcoholic Fatty Liver Disease. *Clin. Liver Dis.* **2023**, *27*, 353–362. [CrossRef]
85. Kim, H.Y.; Rosenthal, S.B.; Liu, X.; Miciano, C.; Hou, X.; Miller, M.; Buchanan, J.; Poirion, O.B.; Chilin-Fuentes, D.; Han, C.; et al. Multi-Modal Analysis of Human Hepatic Stellate Cells Identifies Novel Therapeutic Targets for Metabolic Dysfunction-Associated Steatotic Liver Disease. *J. Hepatol.* **2025**, *82*, 882–897. [CrossRef]
86. Tiniakos, D.G.; Anstee, Q.M.; Brunt, E.M.; Burt, A.D. Fatty Liver Disease. In *MacSween's Pathology of the Liver*; Elsevier: Amsterdam, The Netherlands, 2024; pp. 330–401. ISBN 978-0-7020-8228-3.
87. Germano, C.W.; Mega, P.F.; Mattosinho, T.J.A.P.; Dias, L.L.C.; Gestic, M.A.; Utrini, M.P.; Chaim, F.D.M.; Callejas-Neto, F.; Chaim, E.A.; Cazzo, E. Microvesicular Steatosis in Individuals with Obesity: A Histological Marker of Non-Alcoholic Fatty Liver Disease Severity. *Obes. Surg.* **2023**, *33*, 813–820. [CrossRef] [PubMed]
88. Tandra, S.; Yeh, M.M.; Brunt, E.M.; Vuppalanchi, R.; Cummings, O.W.; Ünalp-Arida, A.; Wilson, L.A.; Chalasani, N. Presence and Significance of Microvesicular Steatosis in Nonalcoholic Fatty Liver Disease. *J. Hepatol.* **2011**, *55*, 654–659. [CrossRef]
89. Romualdo, G.R.; Valente, L.C.; Dos Santos, A.C.S.; Grandini, N.A.; Camacho, C.R.C.; Vinken, M.; Cogliati, B.; Hou, D.-X.; Barbisan, L.F. Effects of Glyphosate Exposure on Western Diet-Induced Non-Alcoholic Fatty Liver Disease in Mice. *Environ. Toxicol. Pharmacol.* **2023**, *104*, 104286. [CrossRef]
90. Cobelo-Gómez, S.; García-Formoso, L.; Fernández-Pombo, A.; Lázare-Iglesias, H.; Díaz-López, E.; Prado-Moraña, T.; Rodríguez-Sobrino, L.; Senra, A.; Araújo-Vilar, D.; Sánchez-Iglesias, S. Metabolic-Associated Steatotic Liver Disease and FGF21 Dysregulation in Seipin-Deficient and BSCL2-Associated Celia's Encephalopathy Murine Models. *Int. J. Mol. Sci.* **2025**, *26*, 12037. [CrossRef]
91. Jeong, B.-K.; Choi, W.-I.; Choi, W.; Moon, J.; Lee, W.H.; Choi, C.; Choi, I.Y.; Lee, S.-H.; Kim, J.K.; Ju, Y.S.; et al. A Male Mouse Model for Metabolic Dysfunction-Associated Steatotic Liver Disease and Hepatocellular Carcinoma. *Nat. Commun.* **2024**, *15*, 6506. [CrossRef] [PubMed]
92. Bedossa, P. [Presentation of a grid for computer analysis for compilation of histopathologic lesions in chronic viral hepatitis C. Cooperative study of the METAVIR group]. *Ann. Pathol.* **1993**, *13*, 260–265.
93. Kleiner, D.E.; Brunt, E.M.; Van Natta, M.; Behling, C.; Contos, M.J.; Cummings, O.W.; Ferrell, L.D.; Liu, Y.; Torbenson, M.S.; Unalp-Arida, A.; et al. Design and Validation of a Histological Scoring System for Nonalcoholic Fatty Liver Disease†. *Hepatology* **2005**, *41*, 1313–1321. [CrossRef]
94. Brunt, E.M.; Janney, C.G.; Di Bisceglie, A.M.; Neuschwander-Tetri, B.A.; Bacon, B.R. Nonalcoholic Steatohepatitis: A Proposal for Grading and Staging the Histological Lesions. *Am. J. Gastroenterol.* **1999**, *94*, 2467–2474. [CrossRef]
95. Brunt, E.M.; Kleiner, D.E.; Wilson, L.A.; Belt, P.; Neuschwander-Tetri, B.A. Nonalcoholic Fatty Liver Disease (NAFLD) Activity Score and the Histopathologic Diagnosis in NAFLD: Distinct Clinicopathologic Meanings §Δ. *Hepatology* **2011**, *53*, 810–820. [CrossRef]
96. Bedossa, P.; Poitou, C.; Veyrie, N.; Bouillot, J.-L.; Basdevant, A.; Paradis, V.; Tordjman, J.; Clement, K. Histopathological Algorithm and Scoring System for Evaluation of Liver Lesions in Morbidly Obese Patients. *Hepatology* **2012**, *56*, 1751–1759. [CrossRef] [PubMed]
97. Liang, W.; Menke, A.L.; Driessen, A.; Koek, G.H.; Lindeman, J.H.; Stoop, R.; Havekes, L.M.; Kleemann, R.; Van Den Hoek, A.M. Establishment of a General NAFLD Scoring System for Rodent Models and Comparison to Human Liver Pathology. *PLoS ONE* **2014**, *9*, e115922. [CrossRef] [PubMed]

98. Liss, K.H.H.; McCommis, K.S.; Chambers, K.T.; Pietka, T.A.; Schweitzer, G.G.; Park, S.L.; Nalbantoglu, I.; Weinheimer, C.J.; Hall, A.M.; Finck, B.N. The Impact of Diet-induced Hepatic Steatosis in a Murine Model of Hepatic Ischemia/Reperfusion Injury. *Liver Transpl.* **2018**, *24*, 908–921. [CrossRef] [PubMed]
99. Yan, M.; Cui, Y.; Xiang, Q. Metabolism of Hepatic Stellate Cells in Chronic Liver Diseases: Emerging Molecular and Therapeutic Interventions. *Theranostics* **2025**, *15*, 1715–1740. [CrossRef]
100. Yashaswini, C.N.; Qin, T.; Bhattacharya, D.; Amor, C.; Lowe, S.; Lujambio, A.; Wang, S.; Friedman, S.L. Phenotypes and Ontogeny of Senescent Hepatic Stellate Cells in Metabolic Dysfunction-Associated Steatohepatitis. *J. Hepatol.* **2024**, *81*, 207–217. [CrossRef]
101. Ramachandran, P.; Brice, M.; Sutherland, E.F.; Hoy, A.M.; Papachristoforou, E.; Jia, L.; Turner, F.; Kendall, T.J.; Marwick, J.A.; Carragher, N.O.; et al. Aberrant Basement Membrane Production by HSCs in MASLD Is Attenuated by the Bile Acid Analog INT-767. *Hepatol. Commun.* **2024**, *8*, e0574. [CrossRef]
102. Wattacheril, J.J.; Abdelmalek, M.F.; Lim, J.K.; Sanyal, A.J. AGA Clinical Practice Update on the Role of Noninvasive Biomarkers in the Evaluation and Management of Nonalcoholic Fatty Liver Disease: Expert Review. *Gastroenterology* **2023**, *165*, 1080–1088. [CrossRef]
103. Neuberger, J.; Patel, J.; Caldwell, H.; Davies, S.; Hebditch, V.; Hollywood, C.; Hubscher, S.; Karkhanis, S.; Lester, W.; Roslund, N.; et al. Guidelines on the Use of Liver Biopsy in Clinical Practice from the British Society of Gastroenterology, the Royal College of Radiologists and the Royal College of Pathology. *Gut* **2020**, *69*, 1382–1403. [CrossRef]
104. Bassegoda, O.; Olivas, P.; Turco, L.; Mandorfer, M.; Serra-Burriel, M.; Tellez, L.; Kwanten, W.; Laroyenne, A.; Farcau, O.; Alvarado, E.; et al. Decompensation in Advanced Nonalcoholic Fatty Liver Disease May Occur at Lower Hepatic Venous Pressure Gradient Levels Than in Patients with Viral Disease. *Clin. Gastroenterol. Hepatol.* **2022**, *20*, 2276–2286.e6. [CrossRef]
105. Aggarwal, S.N.; Magdaleno, T.; Klocksieben, F.; MacFarlan, J.E.; Goonewardene, S.; Zator, Z.; Shah, S.; Shah, H.N. A Prospective, Head-to-Head Comparison of 2 EUS-Guided Liver Biopsy Needles in Vivo. *Gastrointest. Endosc.* **2021**, *93*, 1133–1138. [CrossRef]
106. Cassidy, F.H.; Yokoo, T.; Aganovic, L.; Hanna, R.F.; Bydder, M.; Middleton, M.S.; Hamilton, G.; Chavez, A.D.; Schwimmer, J.B.; Sirlin, C.B. Fatty Liver Disease: MR Imaging Techniques for the Detection and Quantification of Liver Steatosis. *Radiographics* **2009**, *29*, 231–260. [CrossRef]
107. Pineda, N.; Sharma, P.; Xu, Q.; Hu, X.; Vos, M.; Martin, D.R. Measurement of Hepatic Lipid: High-Speed T2-Corrected Multiecho Acquisition at ^{1}H MR Spectroscopy—A Rapid and Accurate Technique. *Radiology* **2009**, *252*, 568–576. [CrossRef]
108. Heinemann, F.; Gross, P.; Zeveleva, S.; Qian, H.S.; Hill, J.; Höfer, A.; Jonigk, D.; Diehl, A.M.; Abdelmalek, M.; Lenter, M.C.; et al. Deep Learning-Based Quantification of NAFLD/NASH Progression in Human Liver Biopsies. *Sci. Rep.* **2022**, *12*, 19236. [CrossRef]
109. Huang, Q.; Qadri, S.F.; Bian, H.; Yi, X.; Lin, C.; Yang, X.; Zhu, X.; Lin, H.; Yan, H.; Chang, X.; et al. A Metabolome-Derived Score Predicts Metabolic Dysfunction-Associated Steatohepatitis and Mortality from Liver Disease. *J. Hepatol.* **2025**, *82*, 781–793. [CrossRef]
110. Frączek, J.; Sowa, A.; Agopsowicz, P.; Migacz, M.; Dylińska-Kala, K.; Holecki, M. Non-Invasive Tests as a Replacement for Liver Biopsy in the Assessment of MASLD. *Medicina* **2025**, *61*, 736. [CrossRef]
111. Aggarwal, P.; Alkhouri, N. Artificial Intelligence in Nonalcoholic Fatty Liver Disease: A New Frontier in Diagnosis and Treatment. *Clin. Liver Dis.* **2021**, *17*, 392–397. [CrossRef]
112. Goh, G.B.-B.; Leow, W.Q.; Liang, S.; Wan, W.K.; Lim, T.K.H.; Tan, C.K.; Chang, P.E. Quantification of Hepatic Steatosis in Chronic Liver Disease Using Novel Automated Method of Second Harmonic Generation and Two-Photon Excited Fluorescence. *Sci. Rep.* **2019**, *9*, 2975. [CrossRef]
113. Dawod, S.; Brown, K. Non-Invasive Testing in Metabolic Dysfunction-Associated Steatotic Liver Disease. *Front. Med.* **2024**, *11*, 1499013. [CrossRef]
114. Kanwal, F.; Neuschwander-Tetri, B.A.; Loomba, R.; Rinella, M.E. Metabolic Dysfunction–Associated Steatotic Liver Disease: Update and Impact of New Nomenclature on the American Association for the Study of Liver Diseases Practice Guidance on Nonalcoholic Fatty Liver Disease. *Hepatology* **2024**, *79*, 1212–1219. [CrossRef]
115. Graf, M.; Graf, C.; Ziegelmayer, S.; Marka, A.W.; Makowski, M.; Teumer, Y.; Paprottka, P.; Willemsen, N.; Nadjiri, J. Complications of Image-Guided Liver Biopsies: Results of a Nationwide Database Analysis. *PLoS ONE* **2025**, *20*, e0323695. [CrossRef]
116. Ferraioli, G.; Barr, R.G.; Berzigotti, A.; Sporea, I.; Wong, V.W.-S.; Reiberger, T.; Karlas, T.; Thiele, M.; Cardoso, A.C.; Ayonrinde, O.T.; et al. WFUMB Guidelines/Guidance on Liver Multiparametric Ultrasound. Part 2: Guidance on Liver Fat Quantification. *Ultrasound Med. Biol.* **2024**, *50*, 1088–1098. [CrossRef]
117. Tan, Z.X.; Mehta, B.; Kusel, K.; Seow, J.; Zelesco, M.; Abbott, S.; Simons, R.; Boardman, G.; Welman, C.J.; Ayonrinde, O.T. Hepatic Steatosis: Qualitative and Quantitative Sonographic Assessment in Comparison to Histology. *Australas. J. Ultrason. Med.* **2024**, *27*, 179–188. [CrossRef]
118. Shen, L.; Patel, R.; Negrete, L.; Shon, A.; Lemieux, S.; Liang, T.; Altmayer, S.; Jha, P.; Kamaya, A. Qualitative Assessment of Hepatic Steatosis on Modern Grayscale Ultrasound: More Accurate than Previously Thought? *Abdom. Radiol.* **2025**, *50*, 6119–6128. [CrossRef]

119. Ratziu, V.; Hompesch, M.; Petitjean, M.; Serdjebi, C.; Iyer, J.S.; Parwani, A.V.; Tai, D.; Bugianesi, E.; Cusi, K.; Friedman, S.L.; et al. Artificial Intelligence-Assisted Digital Pathology for Non-Alcoholic Steatohepatitis: Current Status and Future Directions. *J. Hepatol.* **2024**, *80*, 335–351. [CrossRef]
120. Yin, H.; Xiong, B.; Yu, J.; Fan, Y.; Zhou, B.; Sun, Y.; Wang, L.; Xu, H.; Zhu, Y. Interoperator Reproducibility of Quantitative Ultrasound Analysis of Hepatic Steatosis in Participants with Suspected MASLD: A Prospective Study. *Eur. J. Radiol.* **2024**, *175*, 111427. [CrossRef]
121. Ferraioli, G.; Monteiro, L.B.S. Ultrasound-Based Techniques for the Diagnosis of Liver Steatosis. *World J. Gastroenterol.* **2019**, *25*, 6053–6062. [CrossRef]
122. Pirmoazen, A.M.; Khurana, A.; El Kaffas, A.; Kamaya, A. Quantitative Ultrasound Approaches for Diagnosis and Monitoring Hepatic Steatosis in Nonalcoholic Fatty Liver Disease. *Theranostics* **2020**, *10*, 4277–4289. [CrossRef]
123. Starekova, J.; Hernando, D.; Pickhardt, P.J.; Reeder, S.B. Quantification of Liver Fat Content with CT and MRI: State of the Art. *Radiology* **2021**, *301*, 250–262. [CrossRef]
124. Webb, M.; Yeshua, H.; Zelber-Sagi, S.; Santo, E.; Brazowski, E.; Halpern, Z.; Oren, R. Diagnostic Value of a Computerized Hepatorenal Index for Sonographic Quantification of Liver Steatosis. *Am. J. Roentgenol.* **2009**, *192*, 909–914. [CrossRef]
125. Zsombor, Z.; Rónaszéki, A.D.; Csongrády, B.; Stollmayer, R.; Budai, B.K.; Folhoffer, A.; Kalina, I.; Győri, G.; Bérczi, V.; Maurovich-Horvat, P.; et al. Evaluation of Artificial Intelligence-Calculated Hepatorenal Index for Diagnosing Mild and Moderate Hepatic Steatosis in Non-Alcoholic Fatty Liver Disease. *Medicina* **2023**, *59*, 469. [CrossRef]
126. Gao, J.; Wilde, B.; Kripfgans, O.D.; Chen, J.; Rubin, J.M. The Effect of Backscatter Anisotropy in Assessing Hepatic Steatosis Using Ultrasound Hepatorenal Index. *J. Ultrasound Med.* **2025**, *44*, 1093–1101. [CrossRef]
127. Gottfriedova, H.; Dezortova, M.; Sedivy, P.; Pajuelo, D.; Burian, M.; Sticova, E.; Snizkova, O.; Honsova, E.; Dolecek, F.; Hajek, M. Corrigendum to "Comparison of Ultrasound to MR and Histological Methods for Liver Fat Quantification". Eur. J. Radiol. 183 (2025) 111931. *Eur. J. Radiol.* **2025**, *185*, 112010. [CrossRef]
128. Cheng, G.; Li, X.; Liang, J.; Akiyama, I.; Qiao, X.; Xue, L.; Ding, H. Head-to-Head Comparison of Dual-Elastography and 2D Shear Wave Elastography for Assessing Steatosis, Fibrosis, and Inflammation in MASLD. *Eur. J. Radiol.* **2026**, *196*, 112673. [CrossRef]
129. Czernuszewicz, T.J.; Wang, Y.; Jiang, L.; Kim, K.; Mikulski, Z.; Aji, A.M.; Rojas, J.D.; Gessner, R.C.; Schnabl, B. Noninvasive Monitoring of Steatotic Liver Disease in Western Diet-Fed Obese Mice Using Automated Ultrasound and Shear Wave Elastography. *Liver Int.* **2025**, *45*, e16141. [CrossRef]
130. Khalid, W.B.; Farhat, N.; Lavery, L.; Jarnagin, J.; Delany, J.P.; Kim, K. Non-Invasive Assessment of Liver Fat in Ob/Ob Mice Using Ultrasound-Induced Thermal Strain Imaging and Its Correlation with Hepatic Triglyceride Content. *Ultrasound Med. Biol.* **2021**, *47*, 1067–1076. [CrossRef] [PubMed]
131. Sha, T.; You, Y.; Miao, X.; Deng, H.; Zhang, W.; Ye, H.; Wang, P.; Zheng, R.; Ren, J.; Yin, T. Sequential Ultrasound Molecular Imaging for Noninvasive Identification and Assessment of Non-Alcoholic Steatohepatitis in Mouse Models. *Liver Res.* **2023**, *7*, 342–351. [CrossRef]
132. Amin, M.N.; Rushdi, M.A.; Marzaban, R.N.; Yosry, A.; Kim, K.; Mahmoud, A.M. Wavelet-Based Computationally-Efficient Computer-Aided Characterization of Liver Steatosis Using Conventional B-Mode Ultrasound Images. *Biomed. Signal Process. Control* **2019**, *52*, 84–96. [CrossRef]
133. De Rosa, L.; L'Abbate, S.; Kusmic, C.; Faita, F. Applications of Deep Learning Algorithms to Ultrasound Imaging Analysis in Preclinical Studies on In Vivo Animals. *Life* **2023**, *13*, 1759. [CrossRef]
134. Hanson, J.; Wu, C.; Hoyt, K. Quantitative Multifrequency Ultrasound Imaging Using Narrowband Pulsing for Tissue Characterization. *Investig. Radiol.* **2026**, *1*, 1–21. [CrossRef]
135. Hirooka, M.; Ogawa, S.; Koizumi, Y.; Yoshida, Y.; Goto, T.; Yasuda, S.; Yamahira, M.; Tamai, T.; Kuromatsu, R.; Matsuzaki, T.; et al. iATT Liver Fat Quantification for Steatosis Grading by Referring to MRI Proton Density Fat Fraction: A Multicenter Study. *J. Gastroenterol.* **2024**, *59*, 504–514. [CrossRef]
136. Wong, R.E.; Tasdelen, B.; Tian, Y.; Hwang, D.; Cui, S.X.; Yuan, L.; Nayak, K.S. In-Vivo Liver Proton Density Fat Fraction Quantification at 0.55 T: A Pilot Study with Comparison against 3 T MRI. *Magn. Reson. Mater. Phy* **2025**, *38*, 949–957. [CrossRef]
137. Mazzola, M.; Cannella, R.; Pilato, G.; Blandino, A.A.; Milazzo, M.; Matteini, F.; Vernuccio, F.; Brancatelli, G. Quantitative Liver MRI Biomarkers: What the Radiologist Should Know. *J. Med. Imaging Interv. Radiol.* **2024**, *11*, 13. [CrossRef]
138. Wibulpolprasert, P.; Subpinyo, B.; Chirnaksorn, S.; Shantavasinkul, P.C.; Putadechakum, S.; Phongkitkarun, S.; Sritara, C.; Angkathunyakul, N.; Sumritpradit, P. Correlation between Magnetic Resonance Imaging Proton Density Fat Fraction (MRI-PDFF) and Liver Biopsy to Assess Hepatic Steatosis in Obesity. *Sci. Rep.* **2024**, *14*, 6895. [CrossRef]
139. Yuan, K.; Liu, Q.; Huangfu, X.; Luo, P.; Wang, C.; Qi, F.; Chen, L.; Qiu, B. Diagnostic Accuracy of Hepatic MRI-PDFF and R2* for the Evaluation of Liver Steatosis and Liver Iron Overload: A Meta-Analysis. *Acad. Radiol.* **2025**, *32*, 6541–6554. [CrossRef]
140. Jiang, X.; Washington, M.K.; Izzy, M.J.; Piantek, G.; Lu, M.; Yan, X.; Gore, J.C.; Xu, J. Noninvasive Assessment of Liver Inflammation in Metabolic Dysfunction Associated Steatohepatitis Using MR Cytometry. *npj Imaging* **2025**, *3*, 17. [CrossRef]

141. Yin, C.; Zhang, H.; Du, J.; Zhu, Y.; Zhu, H.; Yue, H. Artificial Intelligence in Imaging for Liver Disease Diagnosis. *Front. Med.* **2025**, *12*, 1591523. [CrossRef]
142. Peng, X.-G.; Ju, S.; Qin, Y.; Fang, F.; Cui, X.; Liu, G.; Ni, Y.; Teng, G.-J. Quantification of Liver Fat in Mice: Comparing Dual-Echo Dixon Imaging, Chemical Shift Imaging, and 1H-MR Spectroscopy. *J. Lipid Res.* **2011**, *52*, 1847–1855. [CrossRef]
143. Waghorn, P.A.; Ferreira, D.S.; Erstad, D.J.; Rotile, N.J.; Masia, R.; Jones, C.M.; Tu, C.; Sojoodi, M.; Chen, Y.I.; Schlerman, F.; et al. Quantitative, Noninvasive MRI Characterization of Disease Progression in a Mouse Model of Non-Alcoholic Steatohepatitis. *Sci. Rep.* **2021**, *11*, 6105. [CrossRef]
144. Hines, C.D.G.; Agni, R.; Roen, C.; Rowland, I.; Hernando, D.; Bultman, E.; Horng, D.; Yu, H.; Shimakawa, A.; Brittain, J.H.; et al. Validation of MRI Biomarkers of Hepatic Steatosis in the Presence of Iron Overload in the Ob/Ob Mouse. *J. Magn. Reson. Imaging* **2012**, *35*, 844–851. [CrossRef]
145. Xavier, A.; Zacconi, F.; Santana-Romo, F.; Eykyn, T.R.; Lavin, B.; Phinikaridou, A.; Botnar, R.; Uribe, S.; Oyarzún, J.E.; Cabrera, D.; et al. Assessment of Hepatic Fatty Acids during Non-Alcoholic Steatohepatitis Progression Using Magnetic Resonance Spectroscopy. *Ann. Hepatol.* **2021**, *25*, 100358. [CrossRef]
146. Tang, H.; Li, J.; Zinker, B.; Boehm, S.; Mauer, A.; Rex-Rabe, S.; Glaser, K.J.; Fronheiser, M.; Bradstreet, T.; Nakao, Y.; et al. Evaluation of a PEGylated Fibroblast Growth Factor 21 Variant Using Novel Preclinical Magnetic Resonance Imaging and Magnetic Resonance Elastography in a Mouse Model of Nonalcoholic Steatohepatitis. *J. Magn. Reson. Imaging* **2022**, *56*, 712–724. [CrossRef]
147. Xia, H.; Min, Y.; Wang, Y.; Gao, S.; Wang, H.; Yan, F.; Liu, R.; Wang, J.; Gu, X.; Bo, T. Multiparametric MRI Evaluation of Liver Fat and Iron after Glucagon-like Peptide-1 Receptor and Glucagon Receptor Dual-Agonist Treatment in a High-Fat Diet–Induced Mouse Model. *Radiology* **2025**, *316*, e243780. [CrossRef]
148. McLeod, M.; Chang, M.C.; Rushin, A.; Ragavan, M.; Mahar, R.; Sharma, G.; Badar, A.; Giacalone, A.; Glanz, M.E.; Malut, V.R.; et al. Detecting Altered Hepatic Lipid Oxidation by MRI in an Animal Model of MASLD. *Cell Rep. Med.* **2024**, *5*, 101714. [CrossRef]
149. Lavin, B.; Eykyn, T.R.; Phinikaridou, A.; Xavier, A.; Kumar, S.; Buqué, X.; Aspichueta, P.; Sing-Long, C.; Arrese, M.; Botnar, R.M.; et al. Characterization of Hepatic Fatty Acids Using Magnetic Resonance Spectroscopy for the Assessment of Treatment Response to Metformin in an *eNOS*$^{-/-}$ Mouse Model of Metabolic Nonalcoholic Fatty Liver Disease/Nonalcoholic Steatohepatitis. *NMR Biomed.* **2023**, *36*, e4932. [CrossRef]
150. Lister, D.; Blizard, G.; Hosseini, M.; Messer, K.; Wellen, J.; Sirlin, C.B.; Ahrens, E.T. Imaging Non-Alcoholic Fatty Liver Disease Model Using H-1 and F-19 MRI. *Mol. Imaging Biol.* **2023**, *25*, 443–449. [CrossRef]

Disclaimer/Publisher's Note: The statements, opinions and data contained in all publications are solely those of the individual author(s) and contributor(s) and not of MDPI and/or the editor(s). MDPI and/or the editor(s) disclaim responsibility for any injury to people or property resulting from any ideas, methods, instructions or products referred to in the content.